NAVAL POSTGRADUATE SCHOOL
Monterey, California

THESIS

PARAMETER OPTIMIZATION OF SEISMIC ISOLATOR MODELS USING RECURSIVE BLOCK-BY-BLOCK NONLINEAR TRANSIENT STRUCTURAL SYNTHESIS

by

Kevin M. Norton

September 2002

Thesis Advisor: Joshua H. Gordis

REPORT DOCUMENTATION PAGE		*Form Approved OMB No. 0704-0188*
Public reporting burden for this collection of information is estimated to average 1 hour per response, including the time for reviewing instruction, searching existing data sources, gathering and maintaining the data needed, and completing and reviewing the collection of information. Send comments regarding this burden estimate or any other aspect of this collection of information, including suggestions for reducing this burden, to Washington headquarters Services, Directorate for Information Operations and Reports, 1215 Jefferson Davis Highway, Suite 1204, Arlington, VA 22202-4302, and to the Office of Management and Budget, Paperwork Reduction Project (0704-0188) Washington DC 20503.		

1. AGENCY USE ONLY *(Leave blank)*	2. REPORT DATE September 2002	3. REPORT TYPE AND DATES COVERED Master's Thesis	
4. TITLE AND SUBTITLE: Title (Mix case letters) Parameter Optimization of Seismic Isolator Models Using Recursive Block-By-Block Nonlinear Transient Structural Synthesis		**5. FUNDING NUMBERS**	
6. AUTHOR(S) Kevin M. Norton			
7. PERFORMING ORGANIZATION NAME(S) AND ADDRESS(ES) Naval Postgraduate School Monterey, CA 93943-5000		**8. PERFORMING ORGANIZATION REPORT NUMBER**	
9. SPONSORING / MONITORING AGENCY NAME(S) AND ADDRESS(ES) N/A		**10. SPONSORING / MONITORING AGENCY REPORT NUMBER**	
11. SUPPLEMENTARY NOTES The views expressed in this thesis are those of the author and do not reflect the official policy or position of the Department of Defense or the U.S. Government.			
12a. DISTRIBUTION / AVAILABILITY STATEMENT Approved for public release; distribution is unlimited		**12b. DISTRIBUTION CODE**	

ABSTRACT *(maximum 200 words)*

In order to increase building safety under earthquake motions, there has been increasing interest in base isolation with passive isolators. Computer modeling is an important aspect of the building design and evaluation process, but solving for the transient response of large structural systems with localized nonlinearities is computationally demanding. Current finite element programs can rapidly determine normalized mode shapes and natural frequencies of several thousand degree of freedom structures for use in determining the transient response. However, actual computation of the transient response can be very time-consuming and expensive for such large structures. A recently developed convolution algorithm utilizes the Volterra integral in a recursive block-by-block integral equation formulation to efficiently compute the transient response of multi-story, nonlinear, base isolated buildings. This algorithm was utilized in a versatile optimization scheme which determines parameters for both linear and nonlinear mathematical model isolators coupled to a multi-degree of freedom structure. To optimize the isolator parameters, the procedure incorporates modal properties computed from a finite element model of the structure, the earthquake accelogram of interest, and user-defined objective and constraint functions. An example is given of a 4-story, single bay structure subjected to the 1940 El Centro NS excitation.

14. SUBJECT TERMS Optimization, Seismic Isolator, Base Isolation, Nonlinear Dynamic Transient Response, Seismic Response, Volterra Integral, Convolution Integral, Hysteretic Isolator			15. NUMBER OF PAGES 64
			16. PRICE CODE

17. SECURITY CLASSIFICATION OF REPORT Unclassified	18. SECURITY CLASSIFICATION OF THIS PAGE Unclassified	19. SECURITY CLASSIFICATION OF ABSTRACT Unclassified	20. LIMITATION OF ABSTRACT UL

NSN 7540-01-280-5500

THIS PAGE INTENTIONALLY LEFT BLANK

PARAMETER OPTIMIZATION OF SEISMIC ISOLATOR MODELS USING RECURSIVE BLOCK-BY-BLOCK NONLINEAR TRANSIENT STRUCTURAL SYNTHESIS

Kevin M. Norton
Lieutenant, United States Navy
B.S., University of Colorado, 1994

Submitted in partial fulfillment of the
requirements for the degree of

MASTER OF SCIENCE IN MECHANICAL ENGINEERING

from the

NAVAL POSTGRADUATE SCHOOL
September 2002

Author:

Kevin M. Norton

Approved by:

Joshua H. Gordis, Thesis Advisor

Young W. Kwon, Chairman
Department of Mechanical Engineering

iii

THIS PAGE INTENTIONALLY LEFT BLANK

ABSTRACT

In order to increase building safety under earthquake motions, there has been increasing interest in base isolation with passive isolators. Computer modeling is an important aspect of the building design and evaluation process, but solving for the transient response of large structural systems with localized nonlinearities is computationally demanding. Current finite element programs can rapidly determine normalized mode shapes and natural frequencies of several thousand degree of freedom structures for use in determining the transient response. However, actual computation of the transient response can be very time-consuming and expensive for such large structures. A recently developed convolution algorithm utilizes the Volterra integral in a recursive block-by-block integral equation formulation to efficiently compute the transient response of multi-story, nonlinear, base isolated buildings. This algorithm was utilized in a versatile optimization scheme which determines parameters for both linear and nonlinear mathematical model isolators coupled to a multi-degree of freedom structure. To optimize the isolator parameters, the procedure incorporates modal properties computed from a finite element model of the structure, the earthquake accelogram of interest, and user-defined objective and constraint functions. An example is given of a 4-story, single bay structure subjected to the 1940 El Centro NS excitation.

THIS PAGE INTENTIONALLY LEFT BLANK

TABLE OF CONTENTS

LIST OF FIGURES

THIS PAGE INTENTIONALLY LEFT BLANK

ACKNOWLEDGMENTS

I would like to express my sincerest appreciation to Professor Joshua H. Gordis for his assistance, support, and patience in completing this thesis. Without his guidance and understanding, this accomplishment would not have been possible.

THIS PAGE INTENTIONALLY LEFT BLANK

I. INTRODUCTION

The use of earthquake protective systems has increased greatly in the last 30 years with numerous structures around the world being built or retrofitted with seismic isolation systems. Seismic isolation, or base isolation, is a design strategy based on the premise that it is feasible to uncouple a structure from the ground in order to protect it from the damaging effects of earthquake motions [Ref. 1]. The base isolation system provides additional flexibility and damping designed to absorb the earthquake energy and thereby reduce the severity of earthquake attacks on the structure. A basic feature of base isolation systems is that the system restricts large deformations to special components, the isolators, while the building vibrates almost as a rigid body [Ref. 2].

The design process for a structural base isolation system is very challenging due to the inherent randomness of earthquakes as well as regional characteristics such as geology, soil composition, proximity to faults, and potential wind loading effects. The primary goal, of course, is to design the system to best protect the structure and its contents from earthquake attack. In this regard, numerical optimization is an effective tool in obtaining suitable parameters for use in preliminary design efforts, but dynamic analysis of large, complex structures is also computationally demanding. This large computational cost strongly inhibits the iterative procedures required in traditional optimization methods.

However, more efficient techniques have been developed to calculate structural responses. A recently developed convolution algorithm utilizes modal information from a finite element model and the Volterra integral in a recursive block-by-block integral equation formulation (RBBIF) to efficiently compute the transient response of multi-story, nonlinear, base isolated buildings [Ref. 3]. This algorithm is extremely fast and was utilized in a versatile optimization scheme capable of determining parameters for a library of linear and nonlinear mathematical model isolators coupled to a multi-degree of freedom (DOF) structure. Within the optimization procedure, the RBBIF algorithm makes use of time and frequency domain synthesis techniques to rapidly recalculate structural system responses of the finite element model as the parameter design variables are altered with each iteration. To optimize the isolator parameters, the algorithmic

1

procedure incorporates modal properties computed from the finite element model of the structure, the earthquake accelogram of interest, and user-defined objective and constraint functions.

A.   ALGORITHM OVERVIEW

The optimization algorithm described in this paper is very versatile and quite suitable for use in dynamic analysis of structures with localized nonlinearities [Ref. 3]. Base isolation systems essentially uncouple the structure from the ground, so by exploiting the preprocessing capabilities of the program, any unconstrained, free-free finite element model can be used. To determine the transient response using RBBIF, modal properties are first extracted from the free-free finite element structure for use in later function calls.

The program can determine numerous items of interest to designers and planners such as base displacement, top floor acceleration, relative velocity, maximum values for displacement, velocity, and acceleration, and root mean square values for displacement, velocity, and acceleration. In addition, the algorithm can be easily modified to determine other items of interest.

There is also a library of linear and nonlinear mathematical isolator models. Of frequent use in current passive isolation design are the bilinear and Wen hysteretic models. The uplift isolator is modeled as a linear spring per [Ref. 4], but, nonlinearities can also be incorporated into this portion of the program. The library of isolators is discussed further in the paper with an emphasis on the bilinear and Wen elements.

It is possible to input any design earthquake relevant to a particular region of interest. Since the program is very fast, the potential exists to input different design earthquakes to determine if similar isolator parameter values are obtained. Earthquake excitations can also be scaled within the program. Numerous earthquake time histories are available at websites such as [Ref. 5] and [Ref. 6]. The design earthquake used in the later example is the El Centro 1940 North-South (NS) component.

II. EARTHQUAKES

Events such as volcanic activity, explosions, and collapsing cave roofs may cause seismic activity. However, the most important earthquakes from an engineering standpoint are of tectonic origin, or, in other words, those associated with large-scale strains in the crust of the earth [Ref. 7]. Numerous analyses associate slip along geologic faults as a primary mechanism to produce tectonic motions, particularly in areas laced with many faults such as Southern California. Recent tectonic earthquakes have occurred with devastating consequences in Turkey, India, Iraq, Japan, and California.

Earthquakes of magnitude 5.0 or greater on the Richter scale generate ground motions severe enough to cause significant structural damage [Ref. 8]. Regarding structural design, prediction of the applied seismic intensity may be complicated and filled with uncertainties. Structures on competent bedrock are subjected predominantly to the effects of relatively high-frequency, low-amplitude vibrations for relatively short durations. The ground surface in such settings is not likely to suffer permanent deformation or ground failure during an earthquake. Structures on compressible deposits, however, particularly where the water table is high (within 33 feet of the surface), are subjected not only to the effects of relatively low frequency, high amplitude vibrations, but also may be subjected to disruption caused by differential settlement, lateral displacement, or liquefaction [Ref. 9]. This was seen in the damaged structures of the Marina District in San Francisco after the 1989 Loma Prieta earthquake.

A. EARTHQUAKE CHARACTERISTICS

Because earthquake motions are irregular and each earthquake is different from all others, even at a given site, it is important to establish whatever characteristics certain groups of earthquakes may have in common and to then base earthquake-resistant design on these generalizations [Ref. 7]. [Ref. 7] describes four general groups of earthquakes:

1) Practically a single shock. Figure 1 is the East-West (EW) component of the earthquake which occurred in Port Hueneme, California, on March 18, 1957. These occur only at short distances from the epicenter, only on firm ground, and

only for shallow earthquakes. Single shock earthquakes are characterized with moderate magnitudes (5.4–6.2), shallow foci (less than 19 miles), almost unidirectional motion, and a prevalence of short periods of vibration (0.2 seconds or less). This type of earthquake motion is very uncommon.
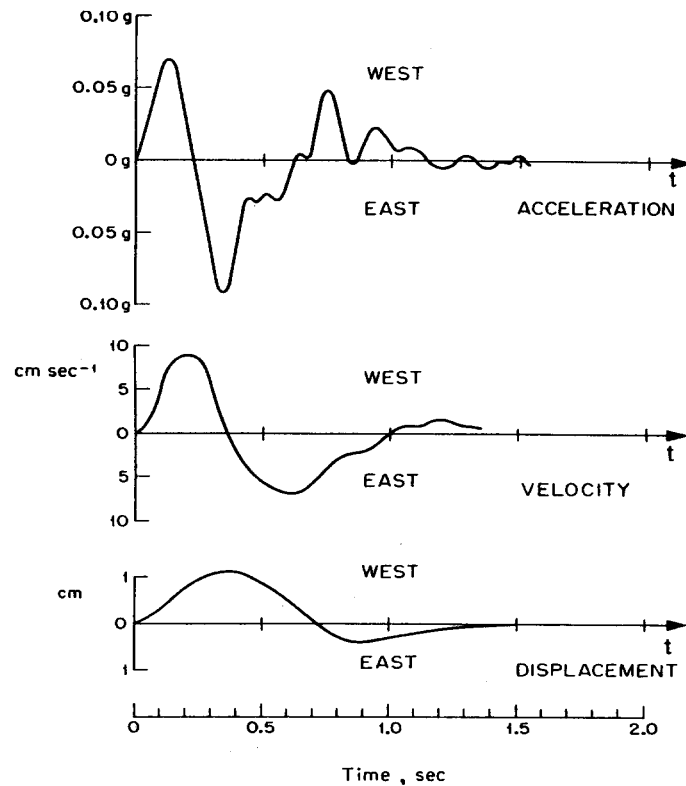
Figure 1. Port Hueneme 1957 EW Component (From: [Ref. 7, p.226])

2) Moderately long, extremely irregular motion. Figure 2 is the North-South (NS) component of the El Centro earthquake which occurred on May 18, 1940. These earthquakes occur at a moderate distance from the epicenter and only on firm ground. Moderately long and irregular earthquakes are characterized by a wide range of vibration periods (0.05-0.5 sec, and 2.5-6 sec) and, ordinarily, equal severity in all directions rather than the unidirectional motion associated with single shock earthquakes. Of note, almost all earthquakes originating along the

4

Circumpacific Belt are of this type, so design earthquakes such as the El Centro 1940 NS component can be applicable for similar geological regions.
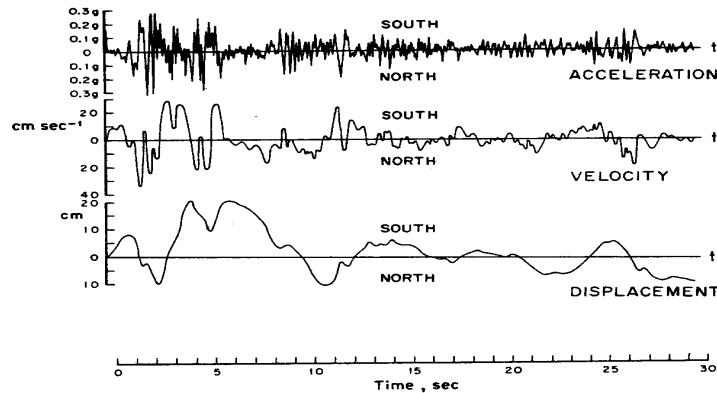
Figure 2. El Centro 1940 NS Component (From: [Ref. 7, p. 227])

3) Long ground motion with pronounced prevailing periods of vibration (e.g., any Mexico City earthquake). Figure 3 is the NS component of the earthquake which occurred in Mexico City on July 6, 1964. This type of earthquake motion results from filtering either (1) a single shock earthquake, or (2) a moderately long earthquake with irregular motion, through layers of soft soil within the range of linear or almost linear soil behavior. These earthquake motions are further amplified by successive wave reflections at the interfaces of these soil mantles.
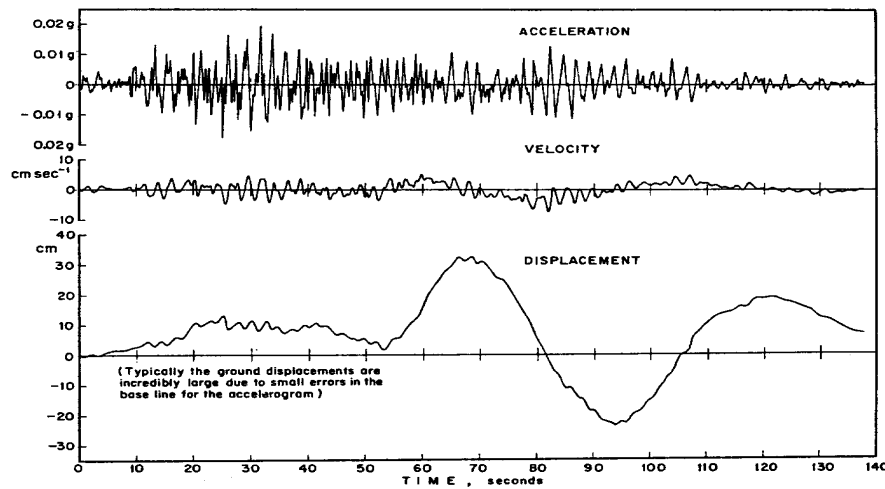
Figure 3. Mexico City 1964 NS Component (From: [Ref. 7, p. 227])

4) Ground motion involving very large-scale, permanent deformations of the ground, with possible slides or soil liquefaction (e.g., Anchorage earthquake of 1964). Ordinarily, it is impractical to attempt a structural design to resist large-scale failure of the ground. In regions where seismic studies indicate this type of motion is probable, it is best to erect the structure at a different site or somehow treat the soil in such a way that the phenomenon becomes unlikely, at least locally.

There are, of course, ground motions with characteristics spanning each of these broad categories, but this classification serves the purpose of outlining general characteristics which may be useful in base isolation design.

B.   DESIGN EARTHQUAKES

General seismic factors which must be considered are local geology and soil properties, proximity to faults, recorded histories of earthquakes in the region, and known or probable characteristics of earthquakes in the region such as intensity or period [Ref.

6

10]. The program works well in these respects since any scaled or actual earthquake time history can be applied to the structural finite element model.

The design earthquakes available from [Refs. 5 and 6] are downloaded in the form of data points. Typical time steps are on the order of 10^{-2}, so each earthquake time history has hundreds of data points. The MATLAB *interp* function is used to interpolate between the points in order to obtain a complete time history for use in the program.

With knowledge of the seismic factors in the region of interest, applicable design earthquake time histories from the previously mentioned website resources can be obtained and applied in the optimization program to determine whether the isolator design parameters remain consistent and suitable for each regional earthquake.

C.   HORIZONTAL AND VERTICAL RESPONSES

The destructive motion in an earthquake is usually the horizontal ground movement [Ref. 11]. Although large vertical components have been recorded in some recent earthquakes, it is felt that these will not usually, of themselves, be destructive but are only a problem if coupling occurs between them and the horizontal components. Such coupling is avoided in the system described in [Ref. 11] by manufacturing bearings with large vertical stiffness and low horizontal stiffness, taking care to ensure the fundamental period of the base isolated building is greater than the periods of the regional design earthquakes.

Although the majority of the destructive ground motion tends to be horizontal, the RBBIF algorithm can efficiently compute both horizontal and vertical structural responses. The development of the structural synthesis is discussed in subsequent sections, and, in the later example, a 4-story finite element structure is subjected, in the horizontal direction, to the frequently used El Centro 1940 NS component design earthquake.

THIS PAGE INTENTIONALLY LEFT BLANK

III. LIBRARY OF SEISMIC ISOLATOR MODELS

As previously mentioned, a library of isolator models is available for use in the program. The library consists of linear and nonlinear mathematical models representing:

1. Linear spring
2. Linear spring and viscous damper in parallel
3. Friction isolator
4. Ideal bilinear element with constant yield stress properties
5. Real bilinear element with changing yield stress properties
6. Maxwell element
7. Wen element

Of frequent use in base isolation design are the bilinear element and the Wen element.   These represent frequency-independent isolators which are capable of maintaining a unique hysteretic loop across a wide range of frequencies. The Maxwell element is also frequency-independent, but it is not studied in this thesis.

Material properties can vary, but, passive isolators known as laminated-rubber bearings can generally be modeled in a linear manner since these have a linear restoring force and linear damping [Ref. 12]. Typical nonlinear passive isolators which could be modeled by the bilinear, Wen, or Maxwell elements are high-damping rubber bearings (HDRB), elastomeric lead-rubber bearings, friction dampers, steel dampers, and lead-extrusion dampers.

A.   HYSTERETIC ISOLATORS

The bilinear element and the Wen element are part of a group collectively referred to as hysteretic isolators. The term, hysteretic, is regarded as frequency-independent damping associated with Coulomb friction at the material grain boundaries, and it also refers to the offset between the loading and unloading curves under cyclic loading or earthquake excitation [Ref. 7]. The bilinear and Wen hysteretic models have gained recognition as accurate and useful tools to numerically portray various structural damping

behaviors. The general nonlinear equation that describes frequency independent isolators is:

$$F = -K_o(1 + i\delta)(x - u_g) \tag{1}$$

where:

K_o - dynamic stiffness

δ - described as the loss factor

x - base motion

u_g - base motion

Hysteretic energy dissipation is one of the most effective means of providing the substantial levels of damping required of a base isolation system. Generally speaking, large displacements can be effectively controlled if additional substantial damping is introduced into the structure through the base isolators. Figure 4 shows an idealized bilinear force-displacement loop where the enclosed area is a measure of the energy dissipated during one cycle of motion. K_1 and K_2 are two distinct stiffness constants, and y_p is the yield-to-post ratio which relates K_1 and K_2. The bilinear model is an approximation to the hysteretic loop shown in Figure 5.
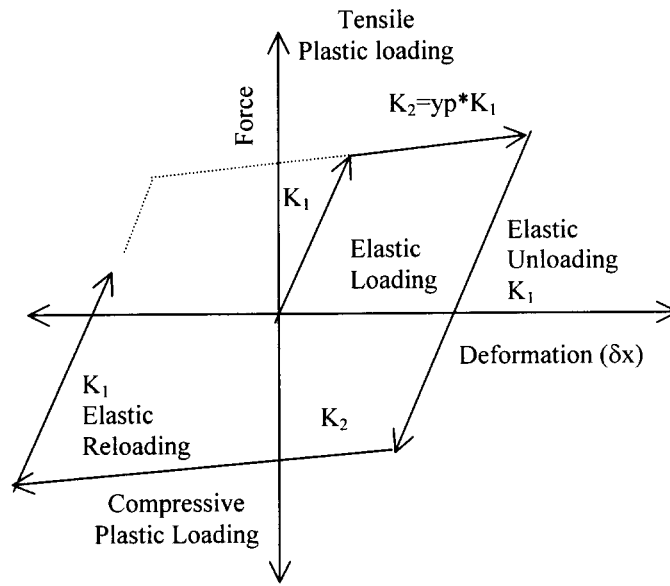
Figure 4. Ideal Bilinear Force-Displacement Loop

In general terms, Equation (1) describes the hysteretic loop shown in Figure 5. The mechanism which forms the hysteretic loop is cyclical deformation along a material's stress-strain curve. Deformation below the tensile and compressive yield stresses describes typical linear elastic behavior. To begin generating the hysteresis loop, deformation occurs beyond the initial yield stress, resulting in plastic deformation. In the plastic region, the material resists additional stress through strain-hardening, which leads to a secondary stiffness rate (K_2 in Figure 4). Unloading from the plastic region occurs elastically until plastic deformation occurs again as the cyclic loading increases. Unloading from the plastic region then occurs elastically again, which completes the hysteretic loop and begins the next cycle.

11
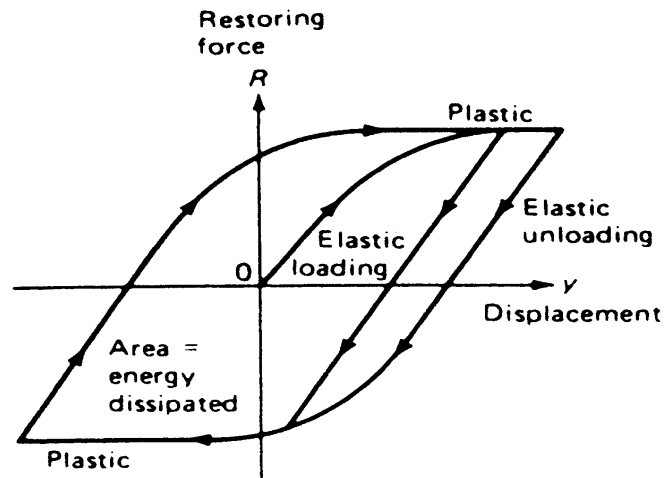
Figure 5. Hysteretic Loop

Examples of rubber isolators which utilize hysteretic energy dissipation to absorb earthquake excitations are the high-damping rubber bearings and elastomeric lead-rubber bearings mentioned previously [Ref. 12].

Rubber bearings such as these are widely used in passive isolation designs. In their basic form, rubber bearings provide vertical support, horizontal flexibility, and centering forces. By inserting additional materials such as carbon black or lead plugs, the hysteretic energy dissipation feature is increased as damping is increased [Refs. 11 and 12].

B.   WEN ELEMENT MODEL

The Wen element is a mathematical equation which accurately models the hysteretic behavior of the previously mentioned nonlinear rubber isolators. The ensuing description is summarized from [Ref. 2].

The Wen nonlinear equation refines the bilinear hysteretic loop from Figure 4 to generate a more realistic hysteresis by varying the parameters of the isolator restoring force, Equation (2):

$$F(t) = \alpha \frac{F_y}{\delta_\gamma} x(t) + (1 - \alpha) F_y z(t) \tag{2}$$

where:

$\alpha \dfrac{F_y}{\delta_\gamma} x(t)$ = equivalent linear portion

$(1 - \alpha) F_y z(t)$ = the nonlinear portion

α = post-to-preyielding stiffness ratio

δ_y = yield displacement of isolator

F_y = yield force of isolator

$z(t)$ = dimensionless hysteretic displacement

z(t) is defined by the nonlinear first order differential equation:

$$\delta_y \dot{z} = -\gamma \left| \dot{x} \right| z \left| z \right|^{\eta - 1} - \beta \dot{x} \left| z \right|^{\eta} + A \dot{x} \tag{3}$$

where:

β, γ, A = dimensionless parameters which control the shape of the hysteresis curve

η = integer which controls smoothness of transition from elastic to plastic

13

The combination of the nonlinear parameters from Equation (3) yields the maximum value of the restoring force.

$$F_{max} = \left[\frac{A}{\gamma + \beta} \right]^{\frac{1}{\eta}}$$

(4)

IV. RECURSIVE BLOCK-BY-BLOCK FORMULATION

The recently developed RBBIF convolution algorithm rapidly computes structural transient responses of a finite element model [Ref. 3]. This rapid analysis capability facilitated development of an efficient and versatile numerical optimization scheme for the design of nonlinear, hysteretic isolators. An overview of the RBBIF formulation is presented here. The complete formulation is covered in [Refs. 3, 14, and 15].

A.   BACKGROUND

Generating the equations of motion of an N-degree of freedom (NDOF) structure allows the structure to be described mathematically both in a static and a dynamic manner. The number of DOF is directly controlled when modeling the structure in a finite element program. By controlling the number of DOF, the number of differential equations describing the structure is then controlled and, hence, computationally manageable. In order to discretize a structure with an infinite number of DOF, a logical determination must first be made with regards to retaining a sufficient number of DOF which sufficiently describe the structure.

Following this step, the structure can then be described by a continuous mathematical model and formulated as a set of partial differential equations (PDE). The PDEs can then be transformed into a set of 2nd order ordinary differential equation (ODE) by using elements of lumped-parameter models. The formulation is covered in structural dynamics textbooks such as [Ref. 8].

Structural synthesis refers to substructure coupling and structural modification in the finite element model. In the context of the physical coordinate synthesis formulations developed in [Refs. 14 and 15], a structural system is defined to consist of one or more uncoupled substructures. A single governing equation for nonlinear transient synthesis was derived in [Ref. 3] which addressed each of the following three general analysis category sets:

1. Structural Modification (m-set) – the addition and/or removal of linear and/or nonlinear structural elements

2. Prescribed Base Motion (b-set) – application of base motion to structure through linear and/or nonlinear elements

3. Substructure Coupling (c-set) – the joining of substructures (a linear analysis)

The "m-set", "b-set", and "c-set" are subsets of DOF associated with structural modification (such as base isolators), prescribed base motion, and substructure coupling, respectively. Each subset may include DOF from all substructures. As reported in [Ref. 14], the nonlinear elements are installed in the synthesis. Consequently, all the substructures are linear, and coupling is also a linear synthesis.

Substructure coupling allows nonlinear elements to be isolated by division of the system into substructures. This feature of the program results in significant computational savings since the eigensolutions of the linear substructures are only solved once. Within the optimization program, the coupling set, or c-set, is of primary interest since this defines the set of DOF subjected to the nonlinear earthquake excitation.

Each substructure is described by impulse response functions calculated at the DOF where nonlinear elements are to be installed, where loads are applied, and at other DOF for which synthesized nonlinear transient response is required.

For the linear substructures, the IRF are most efficiently calculated using modal superposition as described in [Ref. 8]. In order to decrease computational cost, however, the RBBIF algorithm only utilizes a sufficient number of modes to ensure convergence of the IRF within a specified tolerance. These converged IRF are virtually indistinguishable from the "exact" IRF, as shown in [Ref. 14].

B. GOVERNING EQUATIONS

The discretized finite element structural equation of motion, assuming proportional structural damping, is:

$$[M]_{nxn}\left\{\ddot{x}\right\}_{nx1} + [C]_{nxn}\left\{\dot{x}\right\}_{nx1} + [K]_{nxn}\{x\}_{nx1} = \left\{F_{Cset}^{iso}\right\}_{nx1} \qquad (5)$$

where:

n = total number of DOF in the system

16

$\{\, F_{Cset}^{iso}(t)\, \}$ = external isolator restoring forces

The general solution to this second order ordinary differential equation is the sum of the homogeneous and particular solutions:

$$x(t) = x(t)_h + x(t)_p \tag{6}$$

The homogeneous solution for a specific DOF is:

$$x(t)_h = e^{-\zeta \omega_n t}(A\sin\sqrt{1-\zeta}\,\omega_n t + B\cos\sqrt{1-\zeta}\,\omega_n t) \tag{7}$$

The derivation of the particular, or transient, solution depends upon the form of the forcing function. For linear forces, such as those of a linear spring, the solution is attainable through manipulation of Equation (5). However, for nonlinear elements such as hysteretic isolators, the particular solution can be very complex. The particular solution can be obtained by using the governing equation for transient structural synthesis, a nonlinear Volterra integral equation involving a convolution-type kernel. The derivation of this convolution integral is developed in mechanical vibration textbooks such as [Ref. 16], and is formulated as:

$$x(t)_p = \int_{-t}^{t} h(t-\tau)f(\tau)d\tau \tag{8}$$

where:

$f(t)$ = design earthquake time history

$h(t)$ = matrix of impulse response functions (IRF)

C. TIME DOMAIN SYNTHESIS

Substituting the particular solution, Equation (8), into Equation (6) results in the total solution for the general equation of motion written in expanded format here:

$$
\begin{Bmatrix} x_1(t) \\ x_2(t) \\ \vdots \\ \vdots \\ x_m(t) \end{Bmatrix} = \begin{Bmatrix} x_1(t) \\ x_2(t) \\ \vdots \\ \vdots \\ x_m(t) \end{Bmatrix}_h + \int_0^t \begin{bmatrix} h_{11}(t-\tau) & h_{12}(t-\tau) & \cdots & h_{1n}(t-\tau) \\ h_{21}(t-\tau) & h_{22}(t-\tau) & \cdots & h_{2n}(t-\tau) \\ \vdots & \vdots & \cdots & \vdots \\ \vdots & \vdots & \cdots & \vdots \\ h_{n1}(t-\tau) & h_{n2}(t-\tau) & \cdots & h_{nn}(t-\tau) \end{bmatrix} \begin{Bmatrix} F_1^{iso}(\tau) \\ F_2^{iso}(\tau) \\ \vdots \\ \vdots \\ 0 \end{Bmatrix} d\tau \tag{9}
$$

where:

m = number of DOF in the coupling set

n = number of modes

The $\{F_i^{iso}(\tau)\}$ vector components represents the isolator restoring forces resulting from ground excitation on the nodes denoted by the subscript.

To reduce the computational requirements for Equation (9), Equation (5) is transformed into modal space. The linear modal transformation equation is defined as:

$$x_i = \sum_{j=1}^{n} \Phi_i^j q_i^j \tag{10}$$

where:

Φ_i^j = mode shapes

n = number of modes

$i = i^{th}$ mode

$j = j^{th}$ node

By substituting Equation (10) into Equation (5), and then pre-multiplying with the transpose of the mass normalized mode shape matrix, $[\Phi]^{T}$, the modal space equivalent becomes:

$$
\begin{Bmatrix} \ddot{q}_1(t) \\ \ddot{q}_2(t) \\ \vdots \\ \vdots \\ \ddot{q}_n(t) \end{Bmatrix} + \begin{bmatrix} 2\zeta_1\omega_1 & 0 & \cdots & 0 \\ 0 & 2\zeta_2\omega_2 & \cdots & 0 \\ \vdots & \vdots & \cdots & \vdots \\ \vdots & \vdots & \cdots & \vdots \\ 0 & 0 & \cdots & 2\zeta_n\omega_n \end{bmatrix} \begin{Bmatrix} \dot{q}_1(t) \\ \dot{q}_2(t) \\ \vdots \\ \vdots \\ \dot{q}_n(t) \end{Bmatrix} + \begin{bmatrix} \omega_1^2 & 0 & \cdots & 0 \\ 0 & \omega_2^2 & \cdots & 0 \\ \vdots & \vdots & \cdots & \vdots \\ \vdots & \vdots & \cdots & \vdots \\ 0 & 0 & \cdots & \omega_n^2 \end{bmatrix} \begin{Bmatrix} q_1(t) \\ q_2(t) \\ \vdots \\ \vdots \\ q_n(t) \end{Bmatrix} = \begin{bmatrix} \begin{bmatrix} \Phi_1^1 & \Phi_2^1 & \cdots & \Phi_n^1 \end{bmatrix} \\ \begin{bmatrix} \Phi_1^2 & \Phi_2^2 & \cdots & \Phi_n^2 \end{bmatrix} \\ \vdots \\ \begin{bmatrix} \Phi_1^n & \Phi_2^n & \cdots & \Phi_n^n \end{bmatrix} \end{bmatrix} \begin{Bmatrix} F_1(t) \\ F_2(t) \\ \vdots \\ \vdots \\ F_n(t) \end{Bmatrix} \tag{11}
$$

The modal solution of Equation (11) yields the equivalent Volterra integral form of Equation (12):

$$
\begin{Bmatrix} q_1(t) \\ q_2(t) \\ \vdots \\ \vdots \\ q_m(t) \end{Bmatrix} = \begin{Bmatrix} q_1(t) \\ q_2(t) \\ \vdots \\ \vdots \\ q_m(t) \end{Bmatrix}_h + \int_0^t \begin{bmatrix} \tilde{h}_{11}(t-\tau) & 0 & \cdots & 0 \\ 0 & \tilde{h}_{22}(t-\tau) & \cdots & 0 \\ \vdots & \vdots & \cdots & \vdots \\ \vdots & \vdots & \cdots & \vdots \\ 0 & 0 & \cdots & \tilde{h}_{nn}(t-\tau) \end{bmatrix} \begin{bmatrix} \begin{bmatrix} \Phi_1^1 & \Phi_2^1 & \cdots & \Phi_n^1 \end{bmatrix} \\ \begin{bmatrix} \Phi_1^2 & \Phi_2^2 & \cdots & \Phi_n^2 \end{bmatrix} \\ \vdots \\ \begin{bmatrix} \Phi_1^n & \Phi_2^n & \cdots & \Phi_n^n \end{bmatrix} \end{bmatrix} \begin{Bmatrix} F_1^{iso}(\tau) \\ F_2^{iso}(\tau) \\ \vdots \\ \vdots \\ 0 \end{Bmatrix} d\tau \tag{12}
$$

18

Since the system of equations was transformed into modal space the impulse response matrix, [h(t-τ)], is uncoupled and denoted by the (~) symbol. Equation (12) is then transformed back into normal space by multiplying with [φ] and using the modal transformation relationship, Equation (10). This results in:

$$
\begin{Bmatrix} x_1(t) \\ x_2(t) \\ \vdots \\ \vdots \\ x_m(t) \end{Bmatrix} = \begin{Bmatrix} x_1(t) \\ x_2(t) \\ \vdots \\ \vdots \\ x_m(t) \end{Bmatrix}_h + \begin{Bmatrix} \Phi_1^1 \\ \Phi_2^1 \\ \vdots \\ \Phi_n^1 \end{Bmatrix} \begin{Bmatrix} \Phi_1^2 \\ \Phi_2^2 \\ \vdots \\ \Phi_n^2 \end{Bmatrix} \cdots \begin{Bmatrix} \Phi_1^n \\ \Phi_2^n \\ \vdots \\ \Phi_n^n \end{Bmatrix} \int_0^t \begin{bmatrix} \tilde{h}_{11}(t-\tau) & 0 & \cdots & 0 \\ 0 & \tilde{h}_{22}(t-\tau) & \cdots & 0 \\ \vdots & \vdots & \cdots & \vdots \\ 0 & 0 & \cdots & \tilde{h}_{nn}(t-\tau) \end{bmatrix} \begin{bmatrix} \Phi_1^1 & \Phi_2^1 & \cdots & \Phi_n^1 \\ \Phi_1^2 & \Phi_2^2 & \cdots & \Phi_n^2 \\ & & \vdots & \\ \Phi_1^n & \Phi_2^n & \cdots & \Phi_n^n \end{bmatrix} \begin{Bmatrix} F_1^{iso}(\tau) \\ F_2^{iso}(\tau) \\ \vdots \\ 0 \end{Bmatrix} d\tau \quad (13)
$$

where:

m = number of DOF in the coupling subset

n = number of modes

F_i^{iso} = DOF in the coupling subset which are subjected to the excitation force.

Within the RBBIF algorithm, the $F_i^{iso}(\tau)$ components correspond to the seismic isolators.

From Equation (13), it is seen that there are significantly more unknowns than equations. There are (n+m) unknowns and only (n) coupled equations. However, since there are (m) forces in $\{F^{iso}(\tau)\}$, a recursive iteration process can be used on a reduced system of coupled equations which is (m x m) in size. This total solution is written as:

$$
\begin{Bmatrix} x_1(t) \\ x_2(t) \\ \vdots \\ \vdots \\ x_m(t) \end{Bmatrix} = \begin{Bmatrix} x_1(t) \\ x_2(t) \\ \vdots \\ \vdots \\ x_m(t) \end{Bmatrix}_h + \begin{Bmatrix} \Phi_1^1 \\ \Phi_2^1 \\ \vdots \\ \Phi_m^1 \end{Bmatrix} \begin{Bmatrix} \Phi_1^2 \\ \Phi_2^2 \\ \vdots \\ \Phi_m^2 \end{Bmatrix} \cdots \begin{Bmatrix} \Phi_1^n \\ \Phi_2^n \\ \vdots \\ \Phi_m^n \end{Bmatrix} \int_0^t \begin{bmatrix} \tilde{h}_{11}(t-\tau) & 0 & \cdots & 0 \\ 0 & \tilde{h}_{22}(t-\tau) & \cdots & 0 \\ \vdots & \vdots & \cdots & \vdots \\ 0 & 0 & \cdots & \tilde{h}_{nn}(t-\tau) \end{bmatrix} \begin{bmatrix} \Phi_1^1 & \Phi_2^1 & \cdots & \Phi_n^1 \\ \Phi_1^2 & \Phi_2^2 & \cdots & \Phi_n^2 \\ & & \vdots & \\ \Phi_1^m & \Phi_2^m & \cdots & \Phi_n^m \end{bmatrix} \begin{Bmatrix} F_1^{iso}(\tau) \\ F_2^{iso}(\tau) \\ \vdots \\ 0 \end{Bmatrix} d\tau \quad (14)
$$

As previously mentioned, the RBBIF algorithm only retains a specified number of modes, based on a user-defined cutoff frequency, which further reduces the

computational cost. By utilizing this feature and only solving for the DOF in excitation (c-set), the overall result is a large savings in time and computational effort.

D.   RECURSIVE ITERATION

   To further decrease the computational time and effort, a recursive iteration formulation is used. To illustrate the recursive iteration process, an example is given of a nonlinear structure, Figure 6, subjected to excitation, $y(t)$. The nonlinear structure is isolated by two linear springs with respective stiffness coefficients, K_1 and K_2.
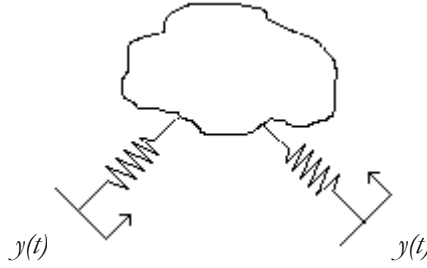

Figure 6. Nonlinear Structure Isolated by Two Linear Springs with K_1, K_2

The isolator restoring forces are: $f_1(t) = K_1\{ x_1(t)-y(t) \}$ (15)

                 $f_2(t) = K_2\{ x_2(t)-y(t) \}$ (16)

Or in matrix form:

$$\{f(t)\} = \begin{bmatrix} K_1 & 0 \\ 0 & K_2 \end{bmatrix} \begin{Bmatrix} x_1(t)-y(t) \\ x_2(t)-y(t) \end{Bmatrix} \tag{17}$$

By using Equation (8), the Volterra convolution integral, to solve for the particular solution, the transient response appears as:

$$\{x(t)\} = \int_0^t H(t-\tau) \begin{bmatrix} K_1 & 0 \\ 0 & K_2 \end{bmatrix} \begin{Bmatrix} x_1(t) - y(t) \\ x_2(t) - y(t) \end{Bmatrix} d\tau \qquad (18)$$

where $H(t\text{-}\tau)$ is known:

$$H(t-\tau) = \begin{bmatrix} H_{11}(t-\tau) & 0 \\ H_{21}(t-\tau) & H_{22}(t-\tau) \end{bmatrix} \qquad (19)$$

which results in Equation (19) after substituting Equation (18):

$$\begin{Bmatrix} x_1(t) \\ x_2(t) \end{Bmatrix} = \int_0^t \begin{bmatrix} H_{11}(t-\tau) & 0 \\ H_{21}(t-\tau) & H_{22}(t-\tau) \end{bmatrix} \begin{Bmatrix} f_1(t) \\ f_2(t) \end{Bmatrix} d\tau \qquad (20)$$

Since $\{x(t)\}$ and $\{f(t)\}$ are unknown vectors, arbitrary values for components of $\{x(t)\}$ are chosen, and the solution is determined with an iterative process until a user-specified convergence tolerance is met. The iteration procedure is as follows:

1. Select $\{x(t)\}$. Set $\{x_{old}(t)\} = \{x(t)\}$.

2. Use $\{x_{old}(t)\}$ to compute $\{f_{new}(t)\}$ from Equation (17).

3. Solve for $\{x_{new}(t)\}$ with Equation (20), using the $\{f_{new}(t)\}$ calculated in the previous step.

4. Check if $\{x_{new}(t)\}$ - $\{x_{old}(t)\} \le$ convergence tolerance.

5. If convergence tolerance is not met, set $\{x_{old}(t)\} = \{x_{new}(t)\}$.

6. Repeat steps 2-5 until $\{x_{new}(t)\}$ - $\{x_{old}(t)\} \le$ convergence tolerance.

21

E.   RECURSIVE BLOCK-BY-BLOCK SYNTHESIS

Incorporation of a recursive block-by-block time history synthesis further decreases the computational time. To begin with, the entire time history is divided into blocks of time, and a small time step is chosen for use in the convolution integral to determine the time history response over the period of each block. The blocks take advantage of the linear properties of the convolution integral, and the time history responses computed for each block form the complete response over the entire time history.

As a general example, the time history from 0 to t_n is divided into (n) blocks, 0-t_1, t_1-t_2, t_2-t_3, …, t_{n-1}-t_n. The recursive iteration procedure described in the previous section is then performed for each block, and the complete solution is of the form:

$$\int_0^{t_n} H(t-\tau)\{f(\tau)\}\,d\tau = \int_0^{t_1} H(t_1-\tau)\{f(\tau)\}d\tau + \int_{t_1}^{t_2} H(t_2-\tau)\{f(\tau)\}\,d\tau + \ldots$$

$$\ldots + \int_{t_{n-1}}^{t_n} H(t_n-\tau)\{f(\tau)\}\,d\tau \tag{21}$$

For a single DOF, Equation (21) is written in matrix form as:

$$
\begin{Bmatrix} \{x_a\} \\ \{x_b\} \\ \{x_c\} \\ \vdots \\ \{x_n\} \end{Bmatrix} =
\begin{Bmatrix}
\begin{Bmatrix} x(0) \\ x(\Delta t) \\ \vdots \\ x(t_1) \end{Bmatrix} \\
\begin{Bmatrix} x(t_1+\Delta t) \\ \vdots \\ x(t_2) \end{Bmatrix} \\
\begin{Bmatrix} x(t_2+\Delta t) \\ \vdots \\ x(t_3) \end{Bmatrix} \\
\vdots \\
\begin{Bmatrix} \vdots \\ x(t_n) \end{Bmatrix}
\end{Bmatrix} =
\begin{bmatrix}
[H_1] & [0] & [0] & \cdots & [0] \\
[H_1] & [H_2] & [0] & \cdots & [0] \\
[H_1] & [H_2] & [H_3] & \cdots & [0] \\
\vdots & \vdots & \vdots & \ddots & \vdots \\
[H_1] & [H_2] & [H_3] & \cdots & [H_n]
\end{bmatrix}
\begin{Bmatrix}
f(0) \\ f(\Delta t) \\ \vdots \\ f(t_1) \\ f(t_1+\Delta t) \\ \vdots \\ f(t_2) \\ f(t_2+\Delta t) \\ \vdots \\ f(t_3) \\ \vdots \\ \vdots \\ f(t_n)
\end{Bmatrix} \tag{22}
$$

where $H_1 \ldots H_n$ are lower triangular.

22

To simplify, let:

f_a = the forcing function for the first block, where $f_a = \{f(0)...f(t_1)\}$

f_b = the forcing function for the second block, where $f_b = \{f(t_1)...f(t_2)\}$

$\vdots$

f_n = the forcing function for the nth block, where $f_n = \{f(t_{n-1})...f(t_n)\}$

The block-by-block synthesis is completed by carrying out the matrix multiplication and applying the recursive iteration in the following manner:

1. Use recursive iteration procedure for $\{x_a\}$ and $\{f_a\}$ until convergence is reached for $\{x_a\} = [H_1]\{f_a\}$.

2. Use recursive iteration procedure for $\{x_b\}$ and $\{f_b\}$ until convergence is reached for $\{x_b\} = [H_1]\{f_a\} + [H_2]\{f_b\}$, where $[H_1]\{f_a\}$ is now known from step (1).

3. Use recursive iteration procedure for $\{x_c\}$ and $\{f_c\}$ until convergence is reached for $\{x_c\} = [H_1]\{f_a\}+[H_2]\{f_b\}+[H_3]\{f_c\}$, where $[H_1]\{f_a\}$ is known from step (1), and $[H_2]\{f_b\}$ is now known from step (2).

4. Continue until recursive block-by-block synthesis is complete.

For most efficient use of the RBBIF algorithm, the first data point within each block must be correct. It is necessary that the force solution for each block have this correct initial value in order to obtain an accurate time history between blocks. For linear

isolators such as the two springs in the example, the recursive block-by-block iterations are relatively straightforward between the individual blocks.

For nonlinear hysteretic isolators, however, an accurate RBBIF synthesis relies heavily on force solutions from the previously solved block. In order to achieve continuity of the hysteretic isolator response between time blocks, the initial block value is interpolated with a direct quadratic approximation from the last three force solution data points of the previous block shown in Figure 7. A MATLAB Runge-Kutta 4 (RK4), ordinary differential equation solver is used for the interpolation of F_{pred} in Figure 7.
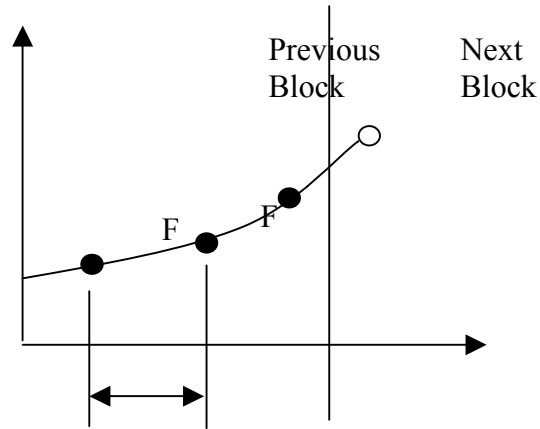
Figure 7. Recursive Interpolation

V. OPTIMIZATION

Base isolation may be used to provide effective solutions for a wide range of seismic design problems. Buildings such as hospitals, fire stations, and police stations must remain in operation at all times, particularly when a disaster such as a major earthquake has caused significant devastation. It is now generally accepted that base isolated buildings will perform better than conventional fixed base buildings in moderate or strong earthquakes [Ref. 17]. There is also a strong economic incentive to incorporate base isolation systems into building design. In addition to minimizing damage from an earthquake, base isolation systems may also lower the overall cost of a structure in terms of less material requirements in the design and decreased insurance rates. Successful implementation of these systems could potentially result in enormous savings of both lives and money, but the design process is challenging.

Numerical optimization can be a useful tool in the design process of base isolators, particularly when making evaluations during the preliminary design phase. The RBBIF method of determining transient structural response is extremely fast and computationally efficient, so its use in an optimization scheme is very appealing.

A.   GENERAL PROBLEM FORMULATION

In an optimization problem, the quantity to be maximized or minimized is the objective function, and the variables to be altered in order to optimize the objective function are termed design variables. The constraint functions are also functions of the design variables, and these can be classified as inequality constraints, equality constraints, or side constraints. In the constrained optimization problem solved by this program, the user defines the objective function and the constraint functions. The objective function is minimized, while ensuring the constraint functions are not violated within a user-defined tolerance. The goal in the formulation of the optimization computer programs is to provide a means of determining optimal values for linear and nonlinear isolator parameters, in order to minimize a dynamic response such as base displacement or top floor acceleration, while simultaneously satisfying all prescribed

constraints. Two minimization problems were studied in this thesis. The first was to minimize the base displacement, and the second was to minimize the top floor acceleration. The general problem formulations follow.

1. First Minimization Problem

The first general optimization problem formulation in the program is:

Minimize: (objective function)

$$f(parameters) = \left\{ \frac{\|x_{Base}(t)\|_\infty}{x_{max}} \right\} = \left\{ \frac{\max_{1 \leq i \leq n} |x_{Base,i}(t)|}{x_{max}} \right\} \tag{23}$$

Ratio of Base Displacement ∞-norm to Maximum Structural Displacement

Subject to: (constraints)

$$\|x_{Base}(t)\|_\infty \leq 0.70 * x_{max} \tag{24}$$

Max Base Displacement ≤ 0.70*Initial Max Structural Displacement

Min Limit ≤ Isolator Parameter Values ≤ Max Limit

Design Variables: Isolator Model Parameters

2. Second Minimization Problem

The second general optimization problem formulation in the program is:

Minimize: (objective function)

$$f(parameters) = \left\{ \frac{\left\| \ddot{x}_{TopFloor}(t) \right\|_\infty}{\ddot{x}_{\max}} \right\} = \left\{ \frac{\max\limits_{1 \le i \le n} \left| \ddot{x}_{TopFloor,i}(t) \right|}{\ddot{x}_{\max}} \right\} \tag{25}$$

Ratio of Top Floor Acceleration ∞-norm to Maximum Structural Acceleration

Subject to: (constraints)

$$\left\| \ddot{x}_{TopFloor}(t) \right\|_\infty \le 0.75 * \ddot{x}_{\max} \tag{26}$$

$$\left\| x_{Base}(t) \right\|_\infty \le 0.70 * x_{\max} \tag{27}$$

Max Top Floor Acceleration ≤ 0.75*Initial Max Structural Acceleration

Max Base Displacement ≤ 0.70*Initial Max Structural Displacement

Min Limit ≤ Isolator Parameter Values ≤ Max Limit

Design Variables: Isolator Model Parameters

B.   MAXIMUM STRUCTURAL DISPLACEMENT

Determining the maximum response of a structure to all possible environmental excitations is a fundamental task in structural dynamics, but the maximum response within a structure may vary from location to location [Ref. 18]. A method reported in [Ref. 19] derives operator norms for the convolution operators associated with linear, time-invariant systems. This method obtains the absolute magnitude of the Euclidean 2 or ∞-norm for the time domain response of a multi-output system to certain classes of input disturbance [Ref. 19]. This method was further refined in [Ref. 18] to determine the maximum response of a structure to an uncertain, vector-valued input, such as an earthquake time history.

Since the RBBIF algorithm is capable of computing nonlinear dynamic response through use of the Volterra convolution integral, results from [Refs. 18 and 19] were incorporated in order to efficiently determine the maximum absolute response of the

entire structure. The complete formulation is found in [Refs. 18 and 19], and the portion used within the algorithm is summarized here.

1. **Linear Operator Norms**

The convolution integral shown in Equation (28) is a linear operator acting on $\{f(t)\}$ to produce $\{x(t)\}$:

$$x(t) = \int_{-t}^{t} h(t-\tau)f(\tau)d\tau \tag{28}$$

where:

$x(t)$ = vector of response outputs

$f(t)$ = applied input design earthquake

$h(t)$ = matrix of impulse responses with each impulse response function defined as:

$$\boldsymbol{h(t)} = \frac{\boldsymbol{x(t)}}{\hat{\boldsymbol{F}}} = \left(e^{-\zeta\omega_n t} \left(\frac{\dot{\boldsymbol{x}}(0) + \zeta\omega_n \boldsymbol{x}(0)}{\omega_n\sqrt{1-\zeta^2}} \sin \omega_n\sqrt{1-\zeta^2}\, t + \boldsymbol{x}(0)\cos \omega_n\sqrt{1-\zeta^2} \right) \right) \tag{29}$$

[Ref. 19] provides the mathematical basis for defining the norm of a vector-valued function of time. For an n-dimensional real-valued vector function $\{x(t)\}$, [Ref. 18] defines the *r*-norm to be:

$$\|x(t)\|_r = \left[\sum_{i=1}^{n} |x_i(t)|^r \right]^{1/r} \tag{30}$$

Normally, only the 2-norm or the ∞-norm are of interest. When *r* is 2, Equation (30) is the Euclidean norm. When *r* is ∞, this is the maximum absolute value component of the vector.

By extending the definition of a vector norm to consider not only the norm across components as a function of time, but the norm across time as well, [Ref. 18] defines the (p,r) norm of the vector-valued function $\{f(t)\}$ to be:

$$\|x\|_{p,r} = \left[\int_{-\infty}^{\infty} \left[\|x(t)\|_r \right]^p dt \right]^{1/p} \tag{31}$$

Of note, Equation (31) does not vary with time. If r approaches 2 and p approaches 2, this norm is the root mean square magnitude. If r approaches ∞ and p approaches ∞, this norm is the maximum value, over all time, of the maximum value of any component in the vector {x(t)} [Ref. 18]:

$$x_{\max} = \|x\|_{\infty,\infty} = \sup_{-\infty \le t \le \infty} \|x(t)\|_\infty = \sup_{-\infty \le t \le \infty} \max |x_i(t)| \tag{32}$$

Equation (31) was incorporated into the optimization algorithm to determine the maximum structural displacement, velocity, and acceleration over all time.

C.   MATLAB OPTIMIZATION TOOLBOX

The optimization tool used in the algorithm is the MATLAB *fmincon* function, which is designed for optimization of a constrained, nonlinear, multivariable problem. Specific, user-oriented instructions are found in the MATLAB Optimization Toolbox, [Ref. 20]. In a constrained optimization problem, the goal is to transform the problem into an unconstrained subproblem that can then be solved and used as the basis of an iterative process. The basis for the subproblem is satisfying the Kuhn-Tucker (KT) conditions, which are necessary conditions for a point, x^*, to be a local minimum. The KT conditions are stated as:

$$\nabla f(x^*) - \sum_{j=1}^{J} u_j \cdot \nabla g_j(x^*) - \sum_{k=1}^{K} v_k \cdot \nabla h_k(x^*) = 0 \tag{33}$$

where:

   $f(x)$ = objective function

   $g(x)$ = inequality constraint functions

   $h(x)$ = equality constraint functions

   u_j = Lagrange multipliers ≥ 0

   v_k = Lagrange multipliers, sign unrestricted

The Lagrange multipliers, u and v, are unspecified parameters which convert the constrained problem into an unconstrained problem. Only active constraints are included in Equation (33), so the inactive constraints are associated with Lagrange multipliers equal to zero. The solution of Equation (33) forms the basis to many nonlinear programming algorithms commonly referred to as Sequential Quadratic Programming (SQP) methods. The *fmincon* function uses SQP methods to determine a search direction for the design variables at every iteration. An overview of the SQP method is found in [Ref. 21], and the optimization algorithm flowchart is shown in Figure 8.
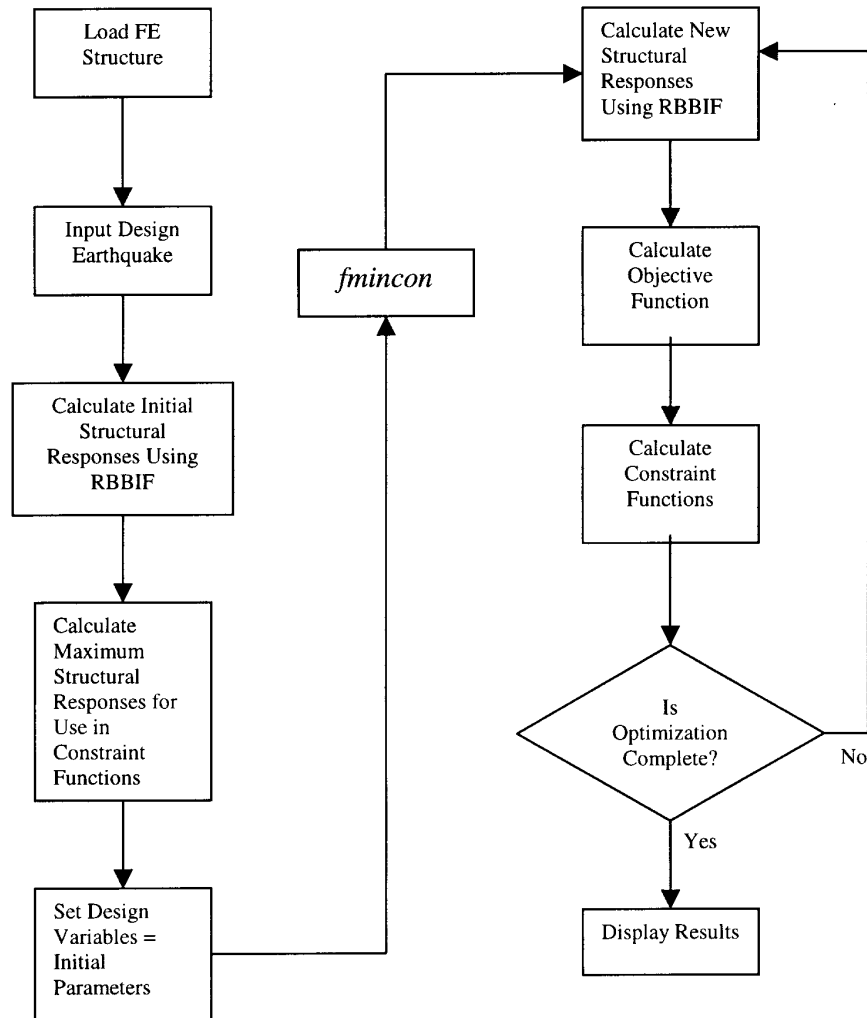
```
┌──────────────┐                                    ┌──────────────┐
│  Load FE     │                                    │ Calculate New│
│  Structure   │                                    │ Structural   │◄──────┐
└──────┬───────┘                                    │ Responses    │       │
       │                                            │ Using RBBIF  │       │
       ▼                                            └──────┬───────┘       │
┌──────────────┐              ┌──────────┐                 │               │
│ Input Design │              │          │                 ▼               │
│ Earthquake   │              │ fmincon  │          ┌──────────────┐       │
└──────┬───────┘              │          │          │ Calculate    │       │
       │                      └────┬─────┘          │ Objective    │       │
       ▼                           │                │ Function     │       │
┌──────────────┐                   │                └──────┬───────┘       │
│ Calculate    │                   │                       │               │
│ Initial      │                   │                       ▼               │
│ Structural   │                   │                ┌──────────────┐       │
│ Responses    │                   │                │ Calculate    │       │
│ Using RBBIF  │                   │                │ Constraint   │       │
└──────┬───────┘                   │                │ Functions    │       │
       │                           │                └──────┬───────┘       │
       ▼                           │                       │               │
┌──────────────┐                   │                       ▼               │
│ Calculate    │                   │                    ╱─────╲            │
│ Maximum      │                   │                  ╱   Is    ╲          │
│ Structural   │                   │                 ◄ Optimization ►──────┘
│ Responses for│                   │                  ╲ Complete? ╱   No
│ Use in       │                   │                    ╲─────╱
│ Constraint   │                   │                       │
│ Functions    │                   │                       │ Yes
└──────┬───────┘                   │                       ▼
       │                           │                ┌──────────────┐
       ▼                           │                │Display Results│
┌──────────────┐                   │                └──────────────┘
│ Set Design   │                   │
│ Variables =  ├───────────────────┘
│ Initial      │
│ Parameters   │
└──────────────┘
```

Figure 8. Optimization Algorithm Flowchart

VI. FINITE ELEMENT BUILDING MODEL USED IN EXAMPLE

In order to demonstrate the capabilities of the program, a finite element model of a 4-story, square base, single bay structure was used. The building is 25 feet wide and has an inter-story height of 17.5 feet. The columns and beams are 50 ksi steel structural members with the following specifications: columns, W36x486; first and second floor beams, W36x170; third floor beams, W36x160; fourth floor beams, W36x150; roof beams, W36x135. Each floor was designed for a 150 psf dead load, and the roof was designed for a 50 psf dead load. The building is modeled with 20 nodes, 120 DOF, and four DOF in excitation in the horizontal direction. A frame illustration of the building is shown in Figure 9.
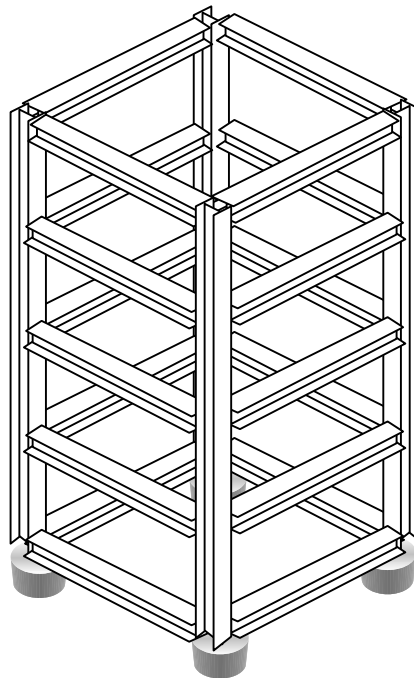
Figure 9. Single Bay, 4-Story Building Frame

The isolators chosen for the example problems are real bilinear element models with the following initial properties, except where noted:

Elastic Stiffness: $k = 15000$ lbf/in

Yield-to-Post Ratio: $y_p = 0.10$

Maximum Tensile Force: $f_{ten} = 25000$ lbf

Maximum Compressive Force: $f_{com} = 30000$ lbf.

The building weight per isolator is 7740 lbf/isolator. The excitation input is the El Centro 1940 NS earthquake component, and a cutoff frequency of 2 Hz was chosen leading to 12 retained modes out of 60 modes total.

VII.   EXAMPLES AND RESULTS

Four examples are presented in which optimal bilinear model parameters are recommended for the 4-story structure subjected, in the horizontal direction, to the El Centro 1940 NS component design earthquake. A Dell Dimension 4100 computer was used to run the optimization program with a time step of 0.05 sec. The primary objective of the first three examples was to reduce the maximum base displacement to 70% of the maximum structural displacement, x_{max}. The initial stiffness value, k, was modified in each example. The primary objective of the last example was to reduce the maximum top floor acceleration to 75% of the maximum structural acceleration, $\ddot{x}_{max}$. The initial parameters for the bilinear isolator model were:

Examples 1 and 4: $k = 15000$ lbf/in

$y_p = 0.10$

$f_{ten} = 25000$ lbf/in

$f_{com} = 30000$ lbf/in

Example 2: $k = 5000$ lbf/in

$y_p = 0.10$

$f_{ten} = 25000$ lbf/in

$f_{com} = 30000$ lbf/in

Example 3: $k = 20000$ lbf/in

$y_p = 0.10$

$f_{ten} = 25000$ lbf/in

$f_{com} = 30000$ lbf/in

A.   GENERAL PROBLEM FORMULATIONS

1.   First Example: Minimize Base Displacement, *k = 15000 lbf/in*

The first optimization problem was to minimize the peak base displacement to less than 70% of the maximum structural displacement. The general optimization formulation was:

Design Variables: Bilinear Model Parameters (k, y_p, f_{ten}, f_{com})

Minimize: $$f(parameters) = \left\{ \frac{\left\| x_{Base}(t) \right\|_\infty}{x_{max}} \right\} = \left\{ \frac{\max\limits_{1 \leq i \leq n} \left| x_{Base,i}(t) \right|}{x_{max}} \right\} \tag{34}$$

Subject to: $$g_1 = \left\| x_{Base}(t) \right\|_\infty \leq 0.70 * x_{max} \tag{35}$$

$$g_2 = 6000 \leq k \leq 25000 \tag{36}$$

$$g_3 = 0.01 \leq y_p \leq 0.40 \tag{37}$$

$$g_4 = 5000 \leq f_{ten} \leq 35000 \tag{38}$$

$$g_5 = -35000 \leq f_{com} \leq -5000 \tag{39}$$

The initial parameters for the bilinear model were:

k = 15000 lbf/in

y_p = 0.10

f_{ten} = 25000 lbf/in

f_{com} = 30000 lbf/in

2.   Results of First Minimization Example

The optimization program recommended the following bilinear model parameters in order to minimize the base displacement response to less than 70% of the initial maximum structural displacement:

k = 13463 lbf/in

y_p = 0.273

f_{ten} = 25392 lbf

f_{com} = 29544 lbf

The minimized objective function value was 0.674, or, in other words, the base displacement was reduced to 67.4% of the initial maximum structural displacement.

The optimization program accomplished this in 33 iterations. Each iteration was approximately 136 seconds, so the program accomplished this within 75 minutes.

Figure 10 shows the base displacements for the initial and the optimized design parameters. The oscillation amplitude is increased on the optimized design even though the overall maximum displacement was decreased. The increased amplitude of the optimized design is probably because the yield-to-post ratio, y_p, increased, which made the secondary stiffness, K_2, larger than the initial design K_2.

Figures 11 and 12 show hysteresis loops for the initial and optimized designs, respectively. The optimized hysteresis loop has much more area enclosed than the initial design. This indicates much more of the earthquake energy was absorbed, resulting in decreased base displacement magnitude.
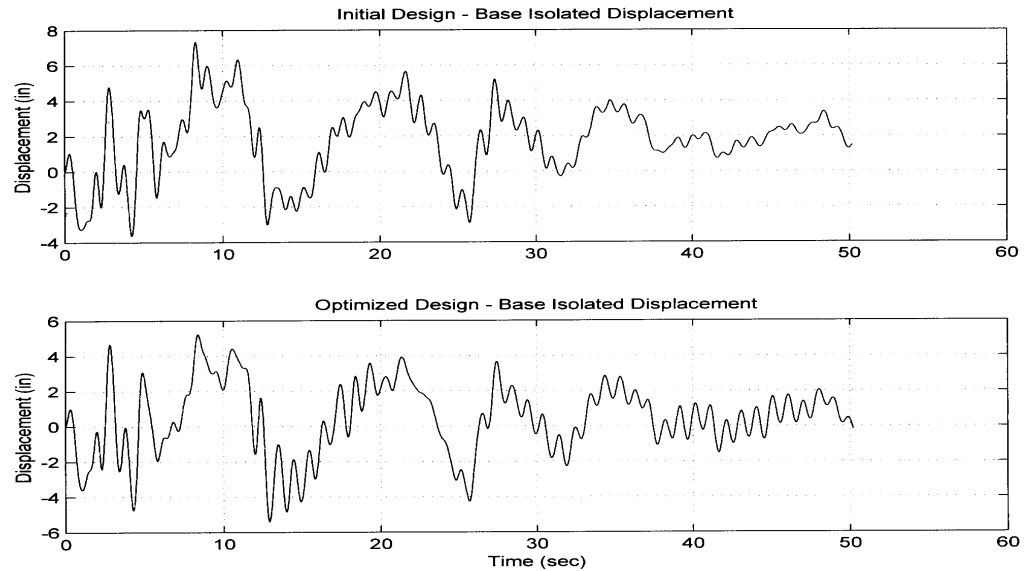
Figure 10. Base Displacement for Initial and Optimized Bilinear Model Parameters
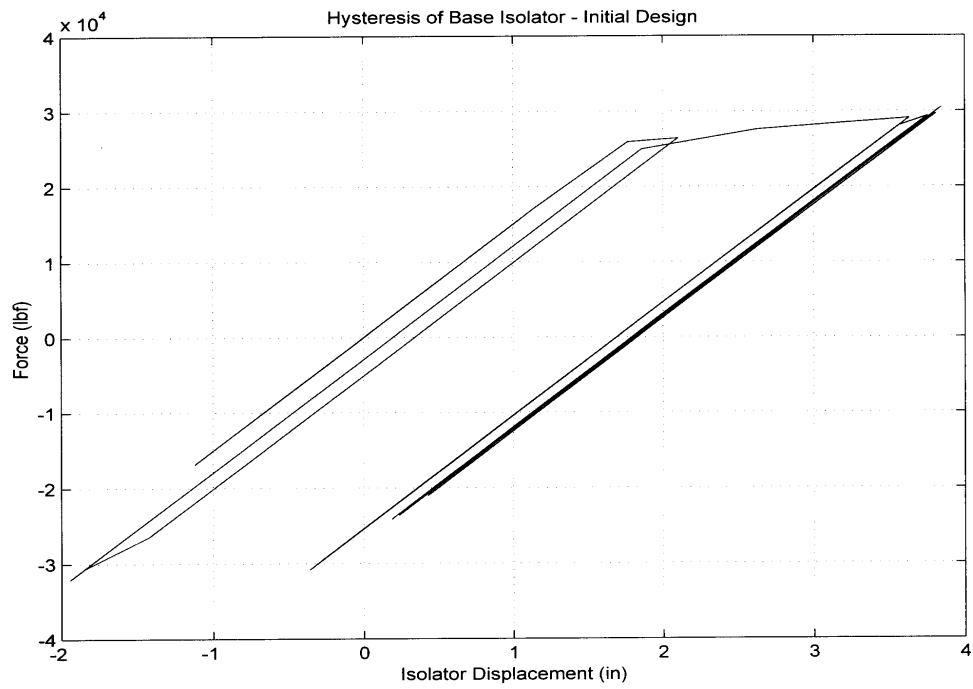
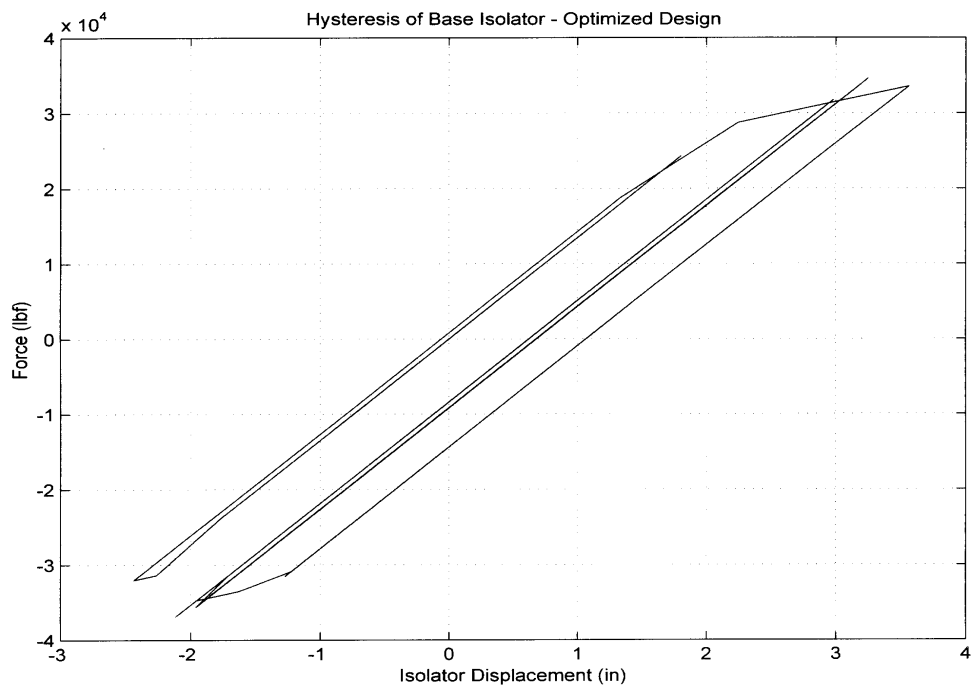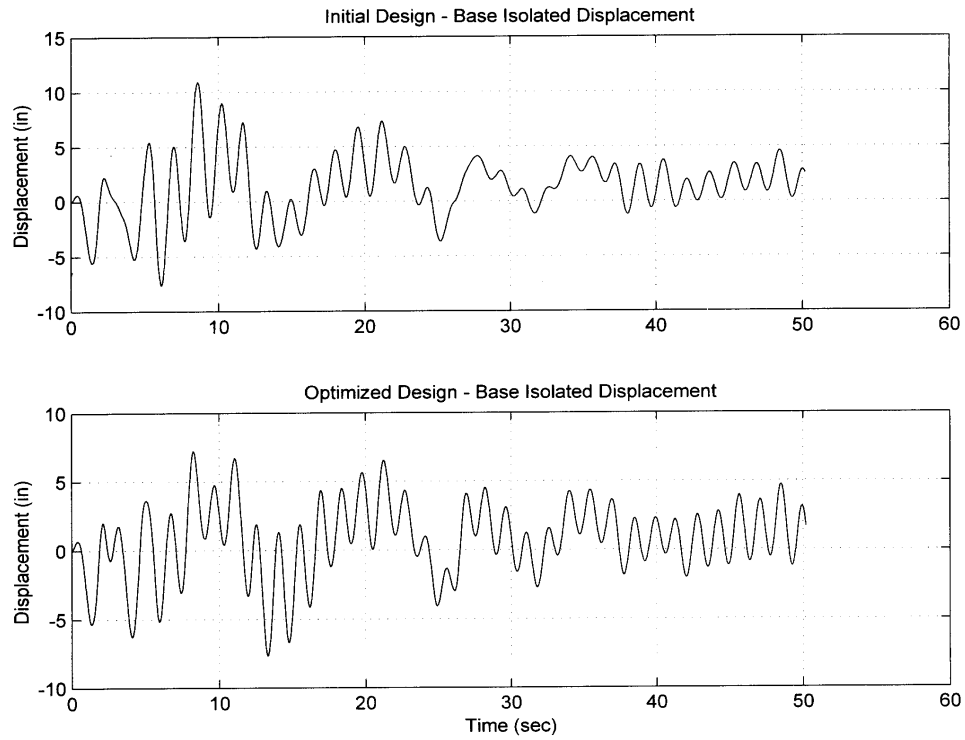Figure 11. Hysteresis Loop for Initial Bilinear Model Parameters

Figure 12. Hysteresis Loop for Optimized Bilinear Model Parameters

36

3.   Second Example: Minimize Base Displacement, *k = 5000 lbf/in*

The second optimization problem was identical to the first: minimize peak base displacement to less than 70% of the maximum structural displacement.

The initial parameters for the bilinear model were:

$k = 5000$ lbf/in

$y_p = 0.10$

$f_{ten} = 25000$ lbf/in

$f_{com} = 30000$ lbf/in

4.   Results of Second Minimization Example

The optimization program recommended the following bilinear model parameters in order to minimize the base displacement response to less than 70% of the initial maximum structural displacement:

$k = 6000$ lbf/in

$y_p = 0.01$

$f_{ten} = 24740$ lbf

$f_{com} = 30004$ lbf

The minimized objective function value was 0.646, or the optimized base displacement was reduced to 67.4% of the initial maximum structural displacement.

The optimization program accomplished this in only 11 iterations. Each iteration was approximately 99 seconds, so the program accomplished this within 18 minutes.

Figure 13 shows the base displacements for the initial and the optimized design parameters.   More oscillations are apparent, and the oscillation amplitude is again increased on the optimized design even though the overall maximum displacement was decreased. This is probably because the stiffness value as well as the yield-to-post ratio are small, resulting in a smaller, more flexible secondary stiffness, K_2.

Figures 14 and 15 show hysteresis loops for the initial and optimized designs, respectively.

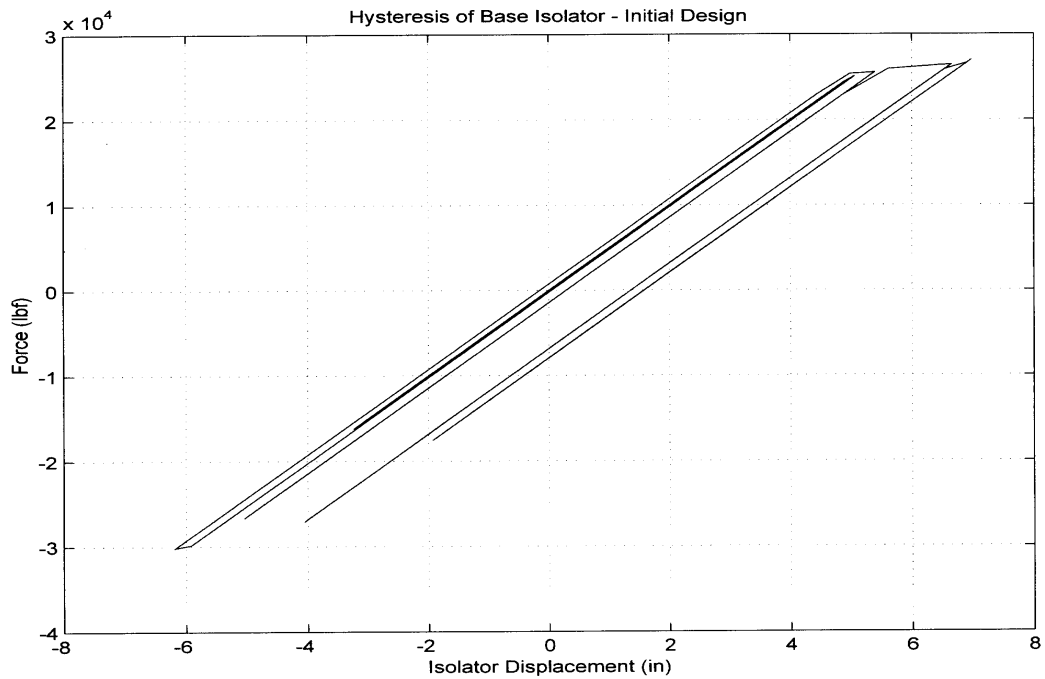Figure 13. Base Displacement for Initial and Optimized Bilinear Model Parameters

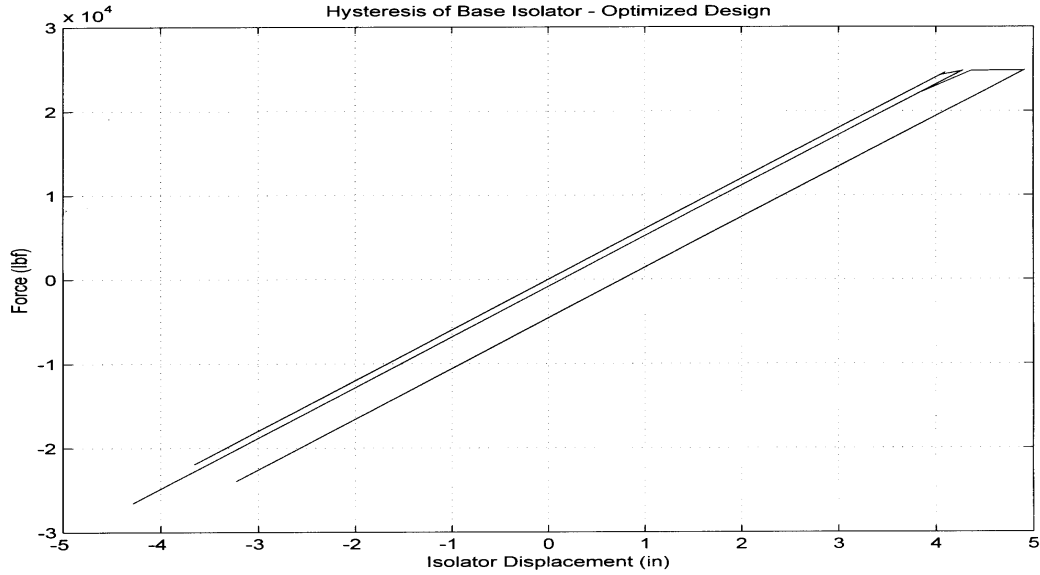Figure 14. Hysteresis Loop for Initial Bilinear Model Parameters

Figure 15. Hysteresis Loop for Optimized Bilinear Model Parameters

5.　　Third Example: Minimize Base Displacement, *k = 20000 lbf/in*

The third optimization problem was also identical to the first: minimize peak base displacement to less than 70% of the maximum structural displacement.

The initial parameters for the bilinear model were:

$k = 20000$ lbf/in

$y_p = 0.10$

$f_{ten} = 25000$ lbf/in

$f_{com} = 30000$ lbf/in

6.　　Results of Third Minimization Example

The optimization program recommended the following bilinear model parameters in order to minimize the base displacement response to less than 70% of the initial maximum structural displacement:

$k = 23271$ lbf/in

$y_p = 0.24$

39

$$f_{ten} = 26434 \text{ lbf}$$

$$f_{com} = 28733 \text{ lbf}$$

The minimized objective function value was 0.697, or the optimized base displacement was reduced to 69.7% of the initial maximum structural displacement.

The optimization program accomplished this in 39 iterations. Each iteration was approximately 174 seconds, so the program accomplished this within 114 minutes.

Figure 16 shows the base displacements for the initial and the optimized design parameters. The large and rapid base displacement oscillations seen in the previous examples are not apparent here. However, the optimized design top floor accelerations seen in Figure 17 are larger than the accelerations from the initial design.

Figures 18 and 19 show hysteresis loops for the initial and optimized designs, respectively.
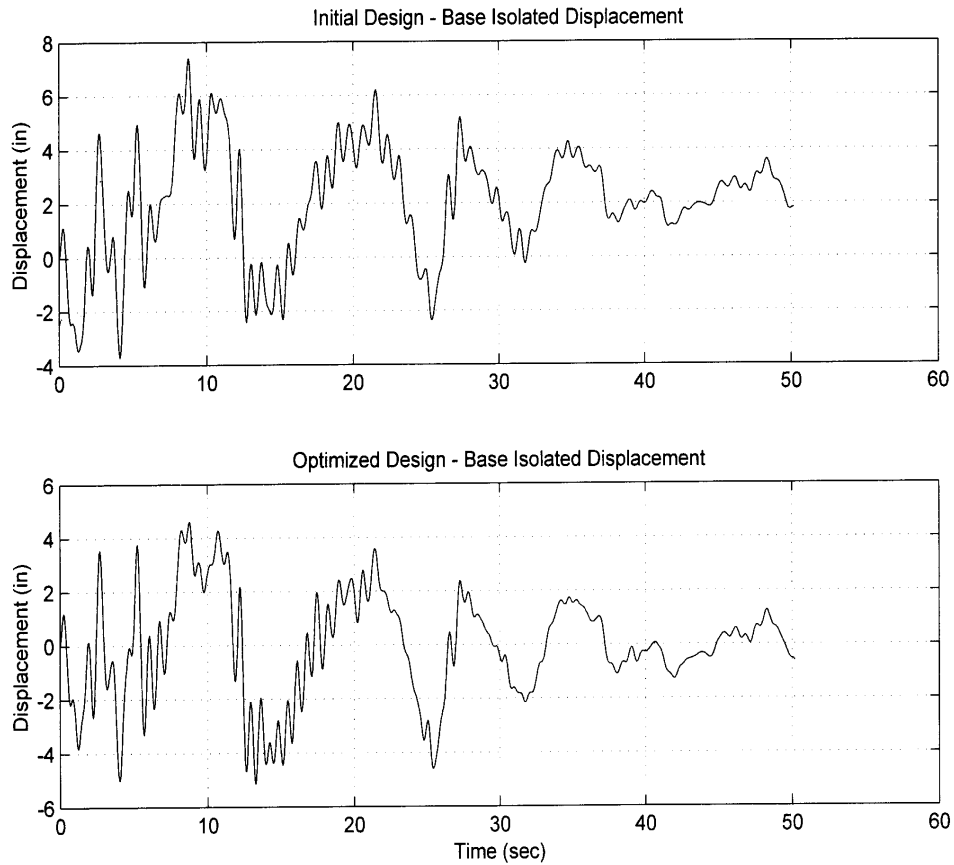

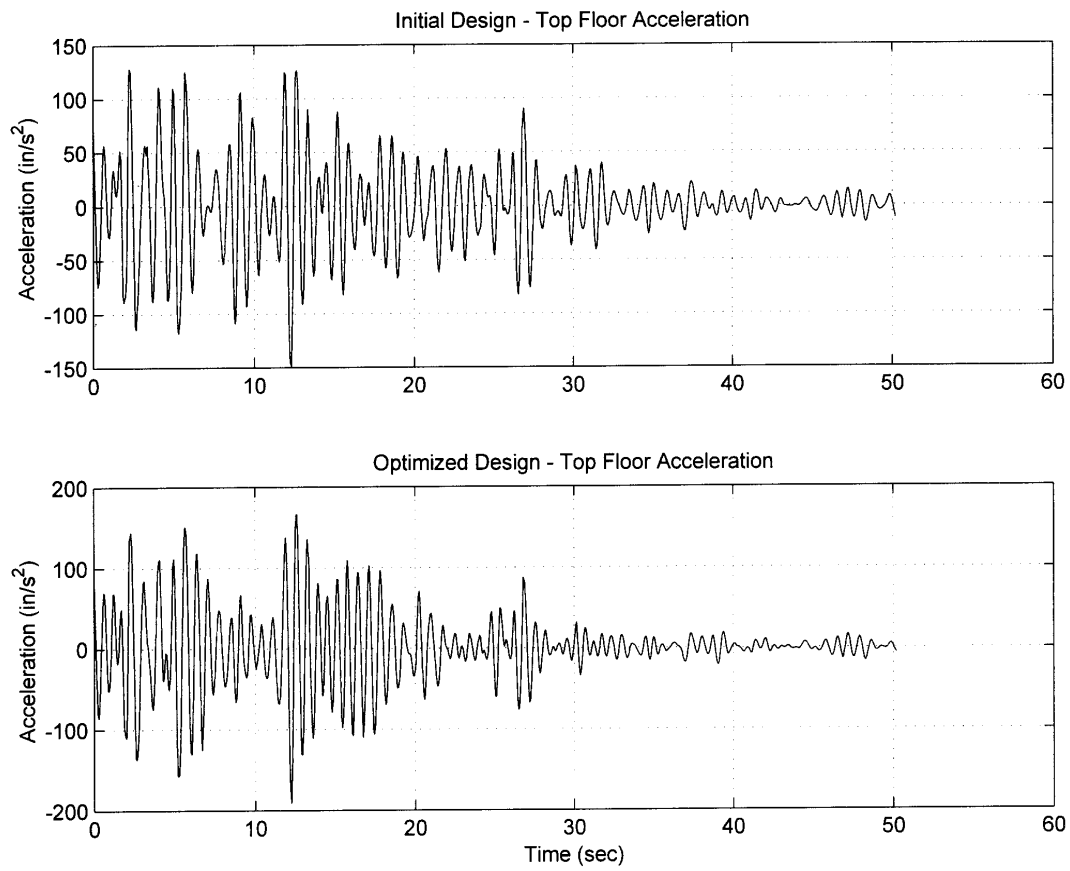Figure 16. Base Displacement for Initial and Optimized Bilinear Model Parameters

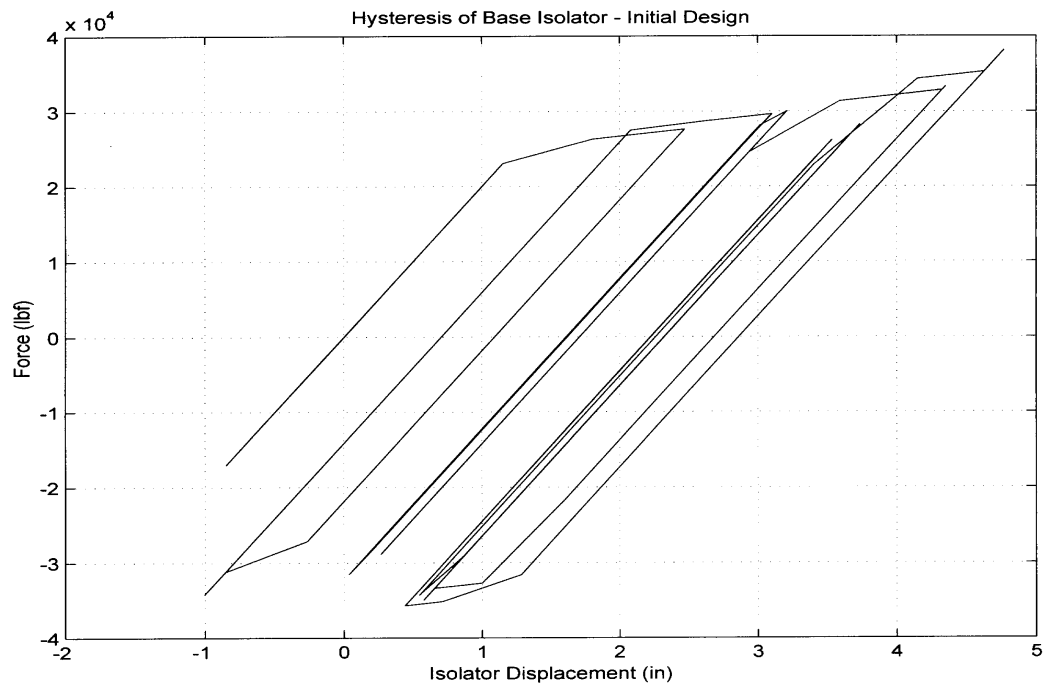Figure 17. Top Floor Acceleration for Initial and Optimized Bilinear Model Parameters

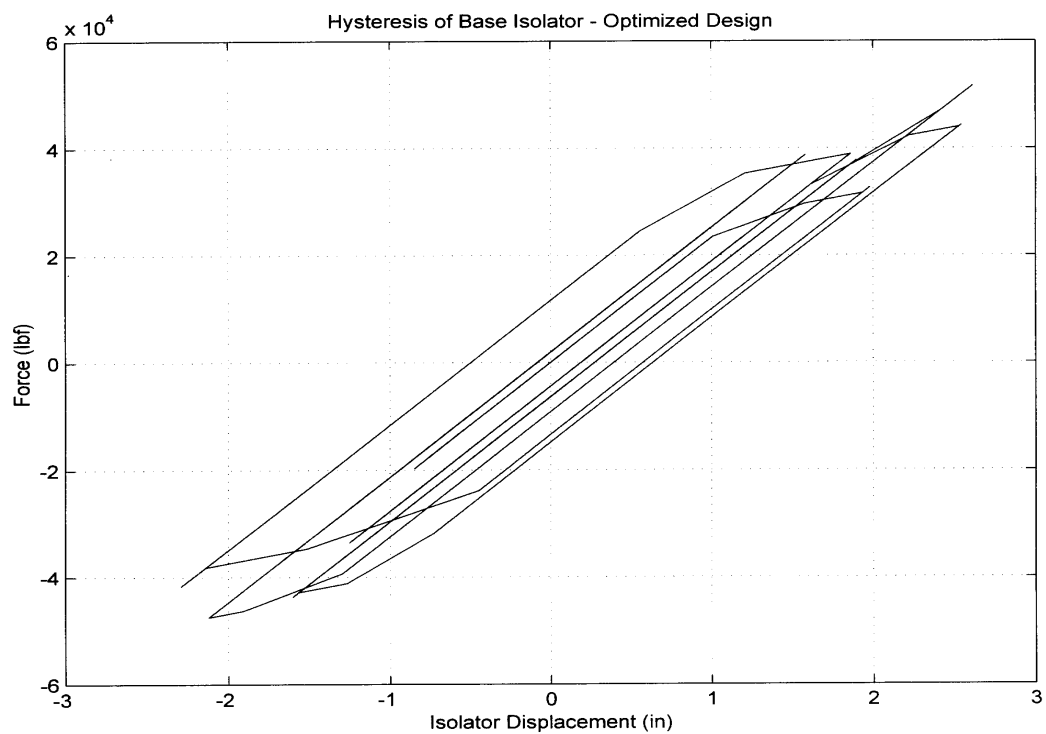Figure 18. Hysteresis Loop for Initial Bilinear Model Parameters

Figure 19. Hysteresis Loop for Optimized Bilinear Model Parameters

42

7. Fourth Example: Minimize Top Floor Acceleration

The second optimization problem was to minimize the peak top floor acceleration to less than 75% of the maximum structural acceleration. The constraint functions from the previous example were maintained, so peak base displacement remained constrained to 70% or less of the maximum structural displacement. The general optimization formulation was:

Design Variables: Bilinear Model Parameters (k, y_p, f_{ten}, f_{com})

$$
\text{Minimize:} \quad f(parameters) = \left\{ \frac{\left\| \ddot{x}_{TopFloor}(t) \right\|_{\infty}}{\ddot{x}_{\max}} \right\} = \left\{ \frac{\max_{1 \le i \le n} \left| \ddot{x}_{TopFloor,i}(t) \right|}{\ddot{x}_{\max}} \right\} \tag{40}
$$

$$
\text{Subject to:} \quad g_1 = \left\| \ddot{x}_{TopFloor}(t) \right\|_{\infty} \le 0.75 * \ddot{x}_{\max} \tag{41}
$$

$$
g_2 = \left\| x_{Base}(t) \right\|_{\infty} \le 0.70 * x_{\max} \tag{42}
$$

$$
g_3 = 6000 \le k \le 25000 \tag{43}
$$

$$
g_4 = 0.01 \le y_p \le 0.40 \tag{44}
$$

$$
g_5 = 5000 \le f_{ten} \le 35000 \tag{45}
$$

$$
g_6 = -35000 \le f_{com} \le -5000 \tag{46}
$$

8. Results of Fourth Minimization Problem

The optimization program recommended the following bilinear model parameters in order to minimize the top floor acceleration response to less than 75% of the initial maximum structural acceleration:

$k = 13096$ lbf/in

$y_p = 0.01$

$f_{ten} = 23232$ lbf/in

$$f_{com} = 22467 \text{ lbf/in}$$

The minimized objective function value was 0.747. The top floor acceleration was reduced to 74.7% of the initial maximum structural acceleration.

The optimization program accomplished this in 36 iterations. Each iteration was approximately 136 seconds, so the program accomplished this within 82 minutes.

Figure 20 shows the top floor accelerations for the initial and the optimized design parameters. Although the maximum top floor acceleration magnitude was decreased by the optimized design, the oscillation amplitude is much larger over the latter portions of the time history. This indicates that larger inertial forces would occur in the structure than would have otherwise occurred with the initial design, even though the maximum acceleration is minimized by the optimized design parameters. This may also indicate the optimized design parameters are not really good, and perhaps a different objective function should be used.

The maximum base displacement for the optimized parameters was also decreased, but the large oscillations seen in the first example did not occur. Figure 21 shows the base displacements for the initial and optimized designs.

Figures 22 and 23 show hysteresis loops for the initial and optimized designs, respectively. Once again, the optimized hysteresis loop has much more area enclosed than the initial design, indicating much more of the earthquake energy was absorbed, and resulting in the decreased top floor acceleration magnitude as well as the decreased base displacement.
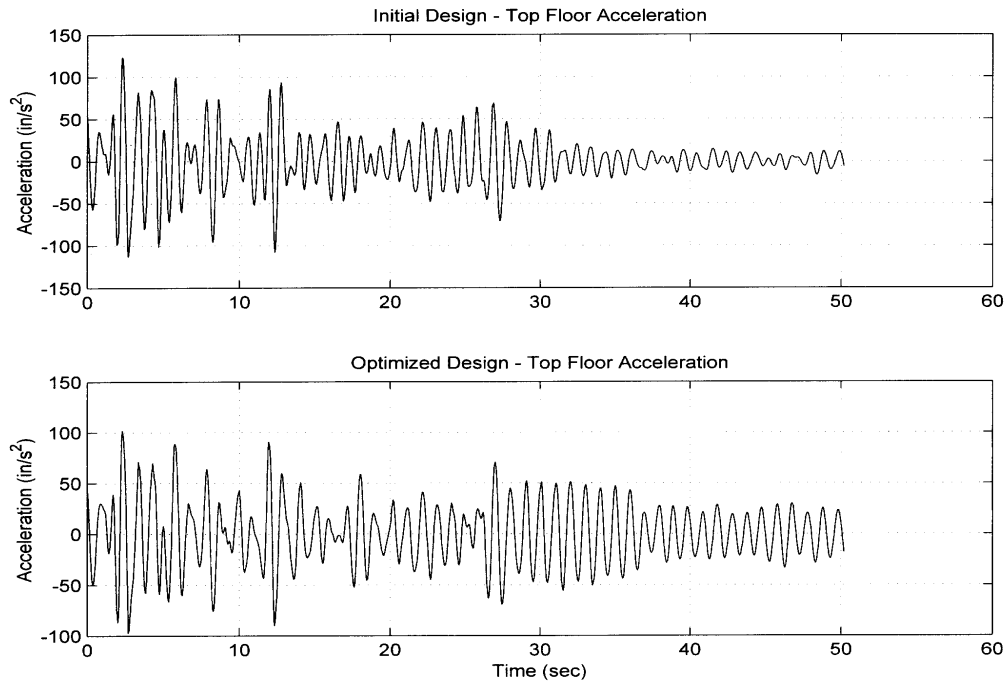
Figure 20. Top Floor Acceleration for Initial and Optimized Bilinear Model Parameters
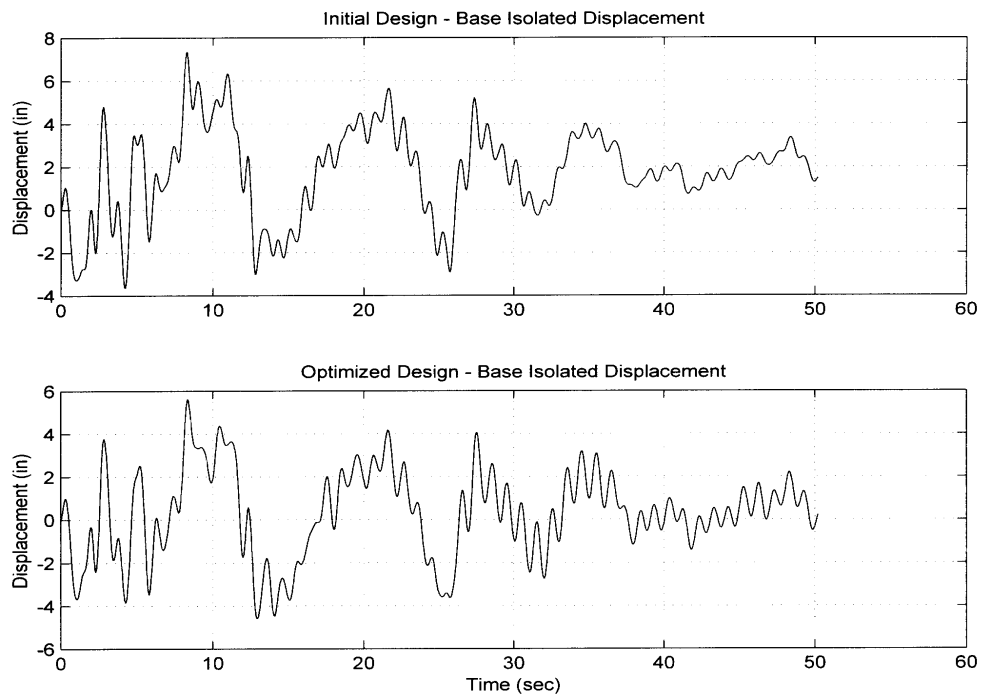

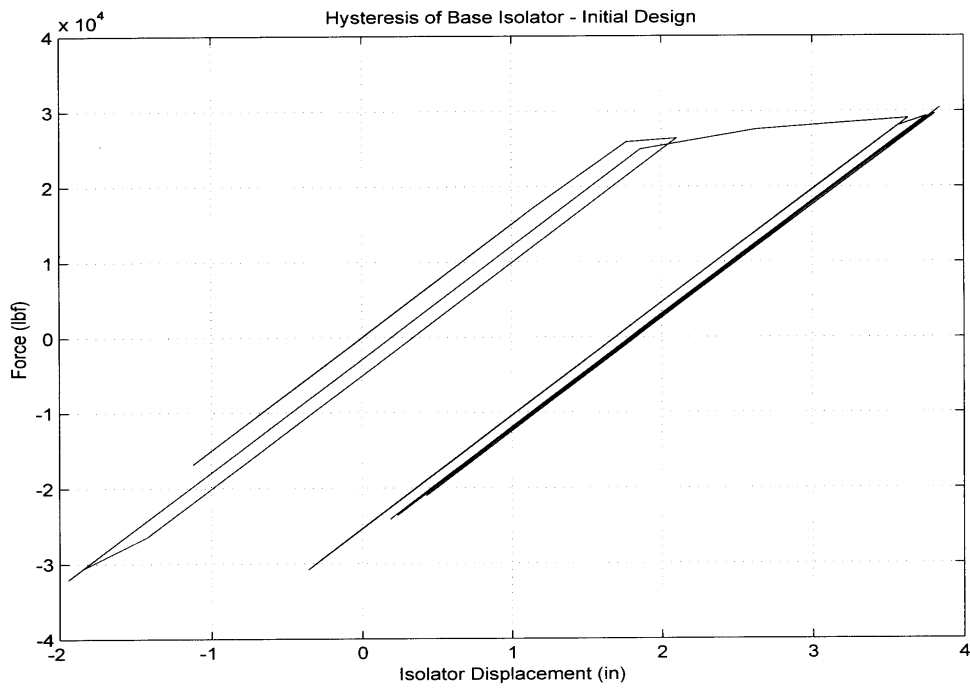Figure 21. Base Displacement for Initial and Optimized Bilinear Model Parameters

45

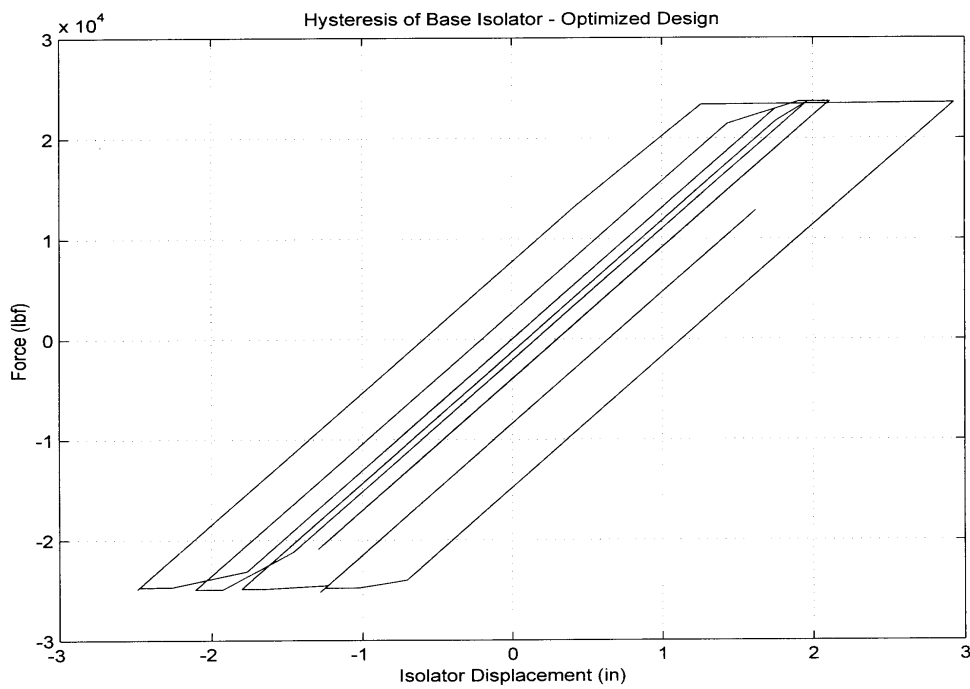Figure 22. Hysteresis Loop for Initial Bilinear Model Parameters

Figure 23. Hysteresis Loop for Optimized Bilinear Model Parameters

46

VIII. CONCLUSION AND RECOMMENDATIONS

A. CONCLUSION

Use of the RBBIF algorithm in an iterative optimization scheme is very appealing. The RBBIF algorithm is very fast, computationally efficient, and capable of determining the transient response of multi-story, nonlinear, base isolated structures. The objective of this thesis was to utilize this algorithm in developing an optimization scheme which determines parameters for a library of linear and nonlinear seismic isolator models. By also utilizing the MATLAB Optimization Toolbox, the computational efficiency of the resulting optimization program was further increased.

The program is also very versatile. Numerous items of design interest can be incorporated into the objective and constraint functions. Both horizontal and vertical responses can be obtained, although one-dimensional analysis is usually the primary concern. In addition, any design earthquake can be used in the program.

The examples show that the optimization program can be very fast. The objective functions in the examples were to minimize peak magnitudes of base displacement and top floor acceleration to some fraction of the initial maximum response. The program accomplished these objectives in a very short time. However, even though the objective function was successfully minimized in each example, parameters were different for each of the first three examples based on the initial starting point. The fourth example also showed that the optimal parameters determined from the user-defined constraints may not actually support a good design.

B. RECOMMENDATIONS FOR FUTURE WORK

The optimization program does not include three-dimensional motion, so further study in this area would be useful in order to validate the program against a real structure and a FE model of that structure. Additionally, the uplift isolator is currently modeled as a linear spring per [Ref. 4], but nonlinearities can be incorporated. There have been studies on two and three-dimensional motion to determine rocking, rolling, and uplift

47

effects on base isolators [Ref. 22]. Information such as this may be useful in developing a nonlinear uplift isolator which can be used for further validation of the program.

LIST OF REFERENCES

1. Buckle, I. G., "Earthquake Protective Systems for Civil Structures," *Proceedings, 10th European Conference on Earthquake Engineering*, vol. 1, p. 641-650, Rotterdam, 1995.

2. Constantinou, M. C. and Tadjbakhsh, I. G., "Hysteretic Dampers in Base Isolation: Random Approach," *Journal of Structural Engineering*, vol. 111, no. 4, pp. 705-721, 1985.

3. Gordis, J. H. and Neta, B., "Efficient Nonlinear Transient Dynamic Analysis for Structural Optimization Using an Exact Integral Equation Formulation," 1999.

4. Lobo, R. F., Naeim, F., and Hart, G. C., "3D Nonlinear Analysis of MultiStory Base Isolated Buildings with Significant Uplift," *Proceedings, 6th U.S. National Conference on Earthquake Engineering*, pp. 1-12, Oakland, CA, 1998.

5. "Strong Motion Database." [http://smdb.crustal.ucsb.edu] September 2001.

6. "PEER Strong Motion Database."   [http://peer.Berkeley.edu/smcat] September 2001.

7. Newmark, N. M and Rosenblueth, E., *Fundamentals of Earthquake Engineering*, Prentice-Hall, Inc., 1971.

8. Craig, R. R., *Structural Dynamics: An Introduction to Computer Methods*, John Wiley & Sons, 1981.

9. Davis, J. F., Bennett, J. H., Borchardt, G. A., Kahle, J. E., Rice, S. J., and Silva, M. A., *Earthquake Planning Scenario for a Magnitude 8.3 Earthquake on the San Andreas Fault in Southern California*, California Department of Conservation, Division of Mines and Geology, 1982.

10. Long, R. E., "The Problem of Estimating Seismic Motions," *Engineering Design for Earthquake Environments*, pp. 59-63, London, 1978.

11. Derham, C. J., Thomas, A. G., and Kelly, J. M., "A Rubber Bearing System for Seismic Protection of Structures," *Engineering Design for Earthquake Environments*, pp. 53-58, London, 1978.

12. Skinner, R. I., Robinson, W. H., and McVerry, G. H., *An Introduction to Seismic Isolation*, John Wiley & Sons, 1993.

13. Kelly, J. M., *Earthquake-Resistant Design with Rubber*, Springer-Verlag London Limited, 1997.

14. Gordis, J. H., "Integral Equation Formulation for Transient Structural Synthesis," *AIAA Journal*, vol. 33, no. 2, pp. 320-324, 1995.

15. Gordis, J. H. and Radwick, J. L. "Efficient Transient Analysis for large Locally Nonlinear Structures," *Shock and Vibration*, vol. 6, no. 1, pp. 1-9, 1999.

16. Thomson, W. T., *Theory of Vibration with Applications*, Prentice Hall, 1993.

17. Kelly, J. M., "The Development of Isolators and Isolation Components for Earthquake-Resistant Design," *Proceedings, 10th European Conference on Earthquake Engineering*, vol. 3, pp. 1863-1868, Rotterdam, 1995.

18. Peterson, L. D., "Bounding the Transient Response of Structures to Uncertain Disturbances," *AIAA Journal*, vol. 34, no. 6, pp1245-1249, 1996.

19. Wilson, D. A., "Convolution and Hankel Operator Norms for Linear Systems," *IEEE Transactions on Automatic Control*, vol. 34, no. 1, pp. 94-97, 1989.

20. Grace, A., *Optimization Toolbox User's Guide*, The Math Works, Inc., 1994.

21. Vanderplaats, G. N., *Numerical Optimization Techniques for Engineering Design*, Vanderplaats Research & Devlopment, Inc., 1999.

22. Koh, A. S. and Hsiung, C. M., "Base Isolation Benefits of 3-D Rocking and Uplift," *Journal of Engineering Mechanics*, vol. 117, no. 1, pp. 1-31, 1991.

INITIAL DISTRIBUTION LIST

1.   Defense Technical Information Center
        Ft. Belvoir, VA

2.   Dudley Knox Library
        Naval Postgraduate School
        Monterey, CA

3.   Engineering & Technology Curricular Office, Code 34
        Naval Postgraduate School
        Monterey, CA

4.   Professor Joshua H. Gordis, Code ME/Go
        Naval Postgraduate School
        Monterey, CA

5.   Commanding Officer, Code C35
        Naval School, Civil Engineer Corps Officers
        Naval Construction Battalion Center
        Port Hueneme, CA

6.   LT Kevin Norton
        Commander, Fleet Activities Yokosuka
        Yokosuka, Japan